Removal of ultrafine particles from indoor environment

Experimental and computational studies of possibilities, limitations and applications

Ardkapan, Siamak Rahimi

Publication date:
2013

Document Version
Early version, also known as pre-print

Removal of ultrafine particles from indoor environment

Experimental and computational studies of possibilities, limitations and applications

Siamak Rahimi Ardkapan

Department of Energy and Environment

Danish Building Research Institute

Aalborg University

Copenhagen, Denmark 2013

Removal of UFPs from indoor environment

Experimental and computational studies of possibilities, limitations and applications

Siamak Rahimi Ardkapan

Main supervisor: Professor Alireza Afshari

Co-supervisor: Professor Peter V. Nielsen

Due to the publication rights of the journals, the five journal articles have been removed from this online version. References are provided within the thesis to the articles.

Paper I. Siamak Rahimi Ardkapan, Alireza Afshari, Niels C. Bergsøe, Peter V. Nielsen. Evaluation of air cleaning technologies existing in the Danish market: Experiments in a duct and in a test room. Online published in *Indoor and Built Environment,* August 2013

Paper II. Siamak Rahimi Ardkapan, Alireza Afshari, Niels C. Bergsøe. Comparing the Performance of a New Electrical Aerosol Detector with other Counters. In the Proceedings of *Indoor Air* conference, 2011

Paper III Siamak Rahimi Ardkapan, Alireza Afshari, Niels C. Bergsøe. Performance and effectiveness of portable air cleaners in an office room: An experimental study. Submitted to *Indoor and Built Environment,* August 2013

Paper IV. Siamak Rahimi Ardkapan, Alireza Afshari, Niels C. Bergsøe, Amalie Gunner, Jasmine Afshari Combining active chilled beams and air cleaning technologies to improve indoor climate in offices: Testing a low pressure mechanical filter in a laboratory environment. Published in ASHRAE *HVAC&R Research*, January 2013. DOI:10.1080/10789669.2013.838440.

Paper V. Siamak Rahimi Ardkapan, Alireza Afshari, Peter V. Nielsen, Ahsan Iqbal, Niels C. Bergsøe. Simulation of particle distribution in a room with air cleaner. In the proceedings of Healthy Building conference, 2012

Paper VI. Siamak Rahimi Ardkapan, Peter V. Nielsen, Alireza Afshari. Studying passive UFP dispersion in a room with a heat source. Published in Building and Environment, 2013. DOI: http://dx.doi.org/10.1016/j.buildenv.2013.09.012.

Paper VII. Siamak Rahimi Ardkapan, Matthew S. Johnson, Sadegh Yazdi, Alireza Afshari, Niels C. Bergsøe. Filtration efficiency of an electrostatic fibrous filter: Studying filtration dependency on UFP exposure and composition. Submitted to Aerosol Science, July 2013

This thesis has been submitted for assessment in partial fulfillment of the PhD degree. The thesis is based on the submitted or published scientific papers which are listed above. Parts of the papers are used directly or indirectly in the extended summary of the thesis. As part of the assessment, co-author statements have been made available to the assessment committee and are also available at the Faculty. The thesis is not in its present form acceptable for open publication but only in limited and closed circulation as copyright may not be ensured.

Summary (English)

In Denmark, people spend most of their time indoors. Therefore, indoor air quality is an important public health issue as people are exposed to pollutants indoors. Pollutants including gases and particles come from outdoors to the inside of a building. They may also be generated indoors by cooking, candle burning, emission from building material, etc. Particles are divided into coarse, fine and ultrafine particles (UFP) depending on their size. Research has indicated that UFPs with diameters less than 100 nanometer (nm) may be harmful to the human body.

Increased ventilation is commonly discussed by researchers as a solution for reducing the particle concentration in the indoor air. Recirculation of air through portable air cleaners has also been discussed.

The scope of this study is to investigate possibilities, applications and limitations of using recirculated air in combination with new air cleaning technologies in order to improve indoor air quality. The objective of this study is to determine the effectiveness of portable air cleaners and to investigate the approaches of using these devices aiming at reducing the concentration of UFPs in the indoor environment.

Experimental investigations and computational fluid dynamics (CFD) simulations were performed parallel in order to investigate the possibilities, limitations and possible applications to reach this aim.

The Danish market was searched for portable air cleaners to be evaluated in the experiments. Five technologies were selected: Non Thermal Plasma, Corona Discharge Ionizer, Portable Air Purifier, Electrostatic Fibrous Filter (EFF) and Three Dimensional Filter. In the experimental investigations, the effectiveness and the generation of by-products of the air cleaners were evaluated, based on measurements performed in a duct, in a clean room and in an unoccupied office building, respectively.

According to the results from the experiments in the clean room, the effectiveness for Non Thermal Plasma, Corona Discharge Ionizer, Portable Air Purifier, EFF and Three Dimensional Filter was 0.2, 0.4, 0.2, 0.7 and 0.5 respectively. The EFF had the highest removal effectiveness. The filter was investigated and it was selected to be combined with a chilled beam. The improvement in UFP removal effectiveness of the combined chilled beam was evaluated.

The simulations were performed using a commercial software STAR-CCM+. Two cases were studied, first the influence of the location of an air cleaner in a room on its UFP removal effectiveness and second, the influence of the height of a heat source and the height of a particle source on the UFP dispersion. The simulated room was based on the dimensions of a laboratory room. Experiments were performed in the laboratory room to validate the predictions by the simulation. According to the experiments performed, comparing the decay rate of UFPs and the decay rate of tracer gas in a room, particles having a diameter smaller than 73 nm had a faster decay rate than the tracer gas. Therefore, if particles are considered as a gas in a CFD simulation or if particles are considered of one single size, a deviation from reality may occur.

It was concluded that an ozone generating air cleaning technology may increase the level of ozone to a level that exceeds the allowed level of 120 μgm^{-3} according to Air Quality Guidelines for Europe provided by World Health Organization. It was also concluded that the maximum ozone concentration in the room and the particle generation rate of reactions between ozone and volatile organic compounds depend mainly on air change rate, the age of the building material and the size of the room.

In addition, it was concluded that the removal efficiency of an electrostatic fibrous filter is directly correlated with UFP concentrations. The reason for this seems to be the formation of chain-like dendrites with electrostatically charged UFPs.

The CFD simulations showed that the location of an air cleaner has a minimal effect on the removal effectiveness in a room with a displacement airflow pattern. According to the simulation study of particle dispersion in a room, it was concluded that the location of a particle source has impact on the UFP concentration profile in the room.

Summary (Danish)

I Danmark opholder mennesker sig en stor del at tiden indendørs. Indeluftens kvalitet er derfor et vigtigt folkesundhedsproblem, idet mennesker udsættes for forureninger indendørs. Forureninger, herunder gasser og partikler, tilføres indeklimaet udefra. Forureninger kan også blive genereret indendørs ved madlavning, tændte stearinlys, emission fra inventar og byggematerialer osv. Partikler inddeles i grove, fine og ultrafine partikler (UFP) afhængig af størrelsen. Forskning har indikeret, at udsættelse for UFPs (diameter mindre end 100 nanometer (nm)) kan indvirke sundhedsskadeligt på den menneskelige krop.

Et almindeligt diskussionsemne blandt forskere er forøget ventilation som middel til at nedbringe koncentrationen af partikler i indeluften. Også recirkulation af luft gennem transportable luftrensere diskuteres.

Fokusområdet for denne undersøgelse er afdækning af muligheder, anvendelsesområder og begrænsninger for anvendelse af recirkulation i kombination med nye luftrensningsteknologier med henblik på forbedring af indeluftkvaliteten. Formålet med undersøgelsen er at bestemme effektiviteten af transportable luftrensere og at undersøge løsningsmetoder for anvendelse af sådanne luftrensere med det formål at reducere koncentrationen af UFPs i indeklimaet.

Eksperimentelle undersøgelser og simuleringer ved hjælp af Computational Fluid Dynamics (CFD) er blevet udført parallelt for at undersøge muligheder, begrænsninger og mulige anvendelsesområder for at nå målet.

Det danske marked med transportable luftrensere blev afsøgt, og fem teknologier blev udvalgt til at indgå i undersøgelserne: Non Thermal Plasma, Corona Discharge Ionizer, Portable Air Purifier, Elektrostatisk Fiber Filter og Tredimensionelt Filter. I de eksperimentelle undersøgelser blev effektiviteten af luftrensere samt genereringen af biprodukter analyseret, på grundlag af målinger udført henholdsvis i en kanal, i et rent rum og i en kontorbygning.

Ifølge resultaterne af eksperimenterne i det rene rum var effektiviteten af Non Thermal Plasma, Corona Discharge Ionizer, Portable Air Purifier, EFF og Tredimensionelt Filter henholdsvis 0.2, 0.4, 0.2, 0.7 and 0.5. EFF havde den højeste effektivitet. Filtret blev undersøgt yderligere og udvalgt til at indgå i kombination med en kølebaffel. Forbedring i effektiviteten af fjernelse af UFP i kombination med kølebaflen blev evalueret.

Simuleringerne blev udført ved hjælp af STAR-CCM +, som er kommercielt tilgængelig software. To situationer blev undersøgt, dels luftrenserens effektivitet i relation til luftrenserens placering i et rum dels indflydelsen af højdeplaceringen af en varmekilde og højdeplaceringen af en partikelkilde på spredningen af UFP. Det simulerede rum var baseret på dimensionerne på et eksisterende rum i laboratoriet. Eksperimenter blev udført i laboratorierummet for at validere resultaterne af simuleringen. Ifølge eksperimenterne, som blev udført med det formål at sammenligne henfald af UFPs med henfald af sporgas i et rum, viser, at partikler, som har en diameter mindre end 73 nm, havde et hurtigere henfald end sporgas. Dette betyder, at såfremt partikler i forbindelse med CFD-simuleringer betragtes som gas eller såfremt partikler antages at være ens i størrelse, kan resultaterne afvige fra virkeligheden.

Det blev konkluderet, at en luftrensningsteknologi, som generer ozon, kan øge niveauet af ozon til et niveau, der overstiger det tilladte niveau, som er 120 µgm-3 i henhold til Air Quality Guidelines

for Europe. Det blev også konkluderet, at den maksimale ozonkoncentration i rummet og raten hvormed partikler blev genereret ved reaktion mellem ozon og flygtige organiske forbindelser primært afhænger af luftskifte, byggematerialernes alder og rumstørrelsen.

Desuden blev det konkluderet, at effektiviteten af et elektrostatisk fiberfilter korrelerer med koncentrationen af ultrafine partikler. Årsagen til dette synes at være dannelse af kædelignende dendritter med elektrostatisk ladede UFPs.

CFD simuleringerne viste, at luftrenserens placering i et rum med fortrængningsventilation har minimal indflydelse på luftrenserens effektivitet. I henhold til simuleringerne af partikelspredning i et rum blev det konkluderet, at partikelkildens placering i rummet har indvirkning på UFP-koncentrationens profil i rummet.

List of Publications

This thesis is based on work reported in the following seven papers.

Paper I. Siamak Rahimi Ardkapan, Alireza Afshari, Niels C. Bergsøe, Peter V. Nielsen. Evaluation of air cleaning technologies existing in the Danish market: Experiments in a duct and in a test room. Online published in *Indoor and Built Environment,* August 2013

Paper II. Siamak Rahimi Ardkapan, Alireza Afshari, Niels C. Bergsøe. Comparing the Performance of a New Electrical Aerosol Detector with other Counters. In the Proceedings of *Indoor Air* conference, 2011

Paper III Siamak Rahimi Ardkapan, Alireza Afshari, Niels C. Bergsøe. Performance and effectiveness of portable air cleaners in an office room: An experimental study. Submitted to *Indoor and Built Environment,* August 2013

Paper IV. Siamak Rahimi Ardkapan, Alireza Afshari, Niels C. Bergsøe, Amalie Gunner, Jasmine Afshari Combining active chilled beams and air cleaning technologies to improve indoor climate in offices: Testing a low pressure mechanical filter in a laboratory environment. Published in ASHRAE *HVAC&R Research*, January 2013. DOI:10.1080/10789669.2013.838440.

Paper V. Siamak Rahimi Ardkapan, Alireza Afshari, Peter V. Nielsen, Ahsan Iqbal, Niels C. Bergsøe. Simulation of particle distribution in a room with air cleaner. In the proceedings of Healthy Building conference, 2012

Paper VI. Siamak Rahimi Ardkapan, Peter V. Nielsen, Alireza Afshari. Studying passive UFP dispersion in a room with a heat source. Published in Building and Environment, 2013. DOI: http://dx.doi.org/10.1016/j.buildenv.2013.09.012.

Paper VII. Siamak Rahimi Ardkapan, Matthew S. Johnson, Sadegh Yazdi, Alireza Afshari, Niels C. Bergsøe. Filtration efficiency of an electrostatic fibrous filter: Studying filtration dependency on UFP exposure and composition. Submitted to Aerosol Science, July 2013

Two following research articles have been published during this PhD research fellowship but are not included in this thesis.

Paper VIII. Conditions for using outdoor-air inlet filter for removing UFP in residential buildings. Alireza Afshari, Siamak Rahimi Ardkapan, Niels Christian Bergsøe, Ahsan Iqbal.
In the proceedings of Healthy Building conference, 2012

Paper IX. Technical solutions for reducing indoor residential exposures to UFPs from second-hand cigarette smoke infiltration. Alireza Afshari, Siamak Rahimi Ardkapan, Niels Christian Bergsøe, Matthew S. Johnson.
In the proceedings of Indoor Air conference, 2011

Preface

The study presented in this thesis was conducted in the department of Energy and Environment at the Danish Building Research Institute of Aalborg University. The thesis is organized as follows: Chapter 1 provides an overall background and identifies the problem and the scope of this study. Chapter 2 describes the methodology of the experiments conducted on the air cleaning technologies and presents the results. Chapter 3 deals with the simulation of UFP dispersion in a room. Chapter 4 comprises discussions of the results. Chapter 5 presents conclusions according to the study. Appendix 1 describes the handling of uncertainty in the experiments, and Appendix 2 explains the method of handling the simulation of the particle phase in the CFD. The last part of thesis is the seven research articles that form the basis for this thesis are.

Here I would like to express my deep appreciation to my main supervisor Professor Alireza Afshari for his kind help, unstinting advice and daily meetings. I have learnt a lot from you about scientific issues and about life. I would like to express my appreciation of the elucidating advice of my supervisor, Professor Peter V. Nielsen, during CFD simulations and advice received about the concepts of fluid dynamics. I express my gratitude to Professor Matthew S. Johnson during stays at Copenhagen University and his generous support and advice during the whole of this study.

I also wish to thank Niels C. Bergsøe for his kind helps during experiments and his precise comments on the reviewed texts. I would like also to thank Solveig Nissen for the language revision of the papers. I want to thank my colleagues in the department of Energy and Environment who have supported me during the years of this research.

I acknowledge also my appreciation to Gabriel Bekö and Sadegh Yazdi from the Technical University of Denmark for their cooperation regarding the experiments. Also, I highly appreciate the cooperation of the companies Lindab AS, Elfi AS, Daikin and Vokes Air AS.

Special thanks to my parents, who have tried to build a better life for me. Thank you my lovely brothers, Babak, Siavash and Arash for your support and encouragements to continue the education.

Maral, I have acknowledged your heartfelt beauty and your pure kindness, and I acknowledge here from deep in my heart, I love you forever. I am sure that without you I could never have completed this study, thank you. You have been supporting me tirelessly during all the hours of the days we have spent together so far, thank you.

Copenhagen, 2013

Errata list

Doctoral candidate: Siamak Rahimi Ardkpan

Titel of thesis: Removal of ultrafine particles from indoor environment, Experimental and computational studies of possibilities, limitations and applications

Abbreviations for different types of corrections:
Cor – correction of language
Cpltf – change of page layout or text format

Page/line/footnote	Original text	(type of correction) Corrected text
24/ 17 /	"The air cleaners were also placed in a duct and connected to a clean room in order to identify and quantify the eventual airborne pollutants generated by them."	(Cor) The air cleaners were tested in the laboratory room. In addition the EFF was also placed in a duct and connected to a clean room in order to identify and quantify the eventual airborne pollutants generated by them"
29 / 9/	"The candle was burnt in the clean room and the air cleaner was connected to the room by a duct."	(Cor) "In addition for the detailed study on EFF, the candle was burnt in the clean room and the air cleaner was connected to the room by a duct."
30 / 6/	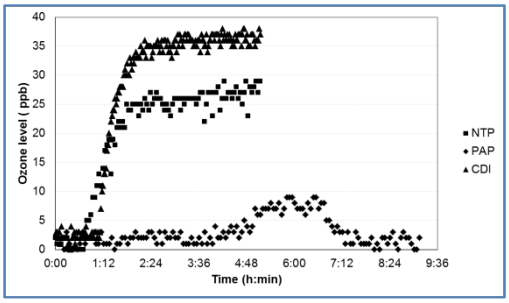 Figure 2.9 Concentration of ozone of the room with air cleaners NTP, PAP and CDI	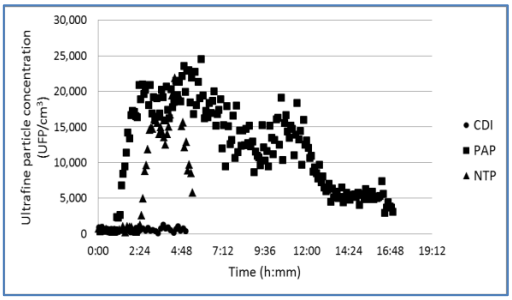 Figure 2.9 UFP concentration of the room with air cleaners CDI, PAP and NTP
38 / 4/	"While *K* is the convective heat factor and a semi-empirical value…"	(Cor) "While *K* is the convective heat factor which is a semi-empirical value…"
41 / 10/	"As is shown in the figure, the Lagrangian approach includes…"	(Cor) "As it is shown in the figure, the Lagrangian approach includes…"
42 / 16/	"…torque exerted on the particle by *M* (Nm) and inertia moment…"	(Cor) "…torque exerted on the particle by *M* (Nms) and inertia moment…"

46 / 5/	“The process the grid-independent solution was repeated…”	(Cor) “The process of grid-independent solution was repeated …”
46 / 18/	“The particle source was located at three heights.”	(Cor) “The particle source was located at two heights.”

Contents

Symbols and Abbreviations

Symbols

$\ddot{x}$	Acceleration of the particle
ω	Angular velocity
C_E	Concentration at exhaust air
C_x	Concentration at location x
C_S	Concentration at supply air
$C_{downstream}$	Concentration, downstream of flow
$C_{upstream}$	Concentration, upstream of flow
P_c	Convective component of heat load
K	Convective heat factor
ε	Effectiveness
EFF	Efficiency
f_b	Fluid force exerted on the particle
u	Fluid velocity at particle location
g	Gravity
H	Heat removal effect
z	Height
Q_f	Induced secondary air flow rate in a chilled beam
I	Inertia moment of the particle
k	Kelvin
k-ε	k-epsilon turbulent model
k-ω	k-omega turbulent model
m_f	Mass of flow displaced because of particle volume
μm	Micrometer
E_f	Particle removal efficiency
λd	Particle removal rate by deposition
λv	Particle removal rate by ventilation system
v	Particle velocity
C_{ctrl}	Pollutant concentration in a room with air cleaner
C_{ref}	Pollutant concentration in a room without air cleaner
f_s	Representative of surface forces

C	Specific heat capacity
ΔT	Temperature difference between supply water and return water
M	Torque exerted on the particle
P_t	Total power of heat source
V	Volume of room
f	Water flow rate

Abbreviations

ACH	Air Change Rate per hour
CO	Carbon monoxide
CADR	Clean Air Delivery Rate
CFD	Computational Fluid Dynamics
CPC	Condensation Particle Counter
CDI	Corona Discharge Ionizer
N_2O	Dinitrogen oxide
EFF	Electrostatic Fibrous Filter
HEPA	High Efficiency Particulate Air
NO_x	Nitrogen Oxides
NTP	Non Thermal Plasma
PDF	Particle Distribution Functions
ppb	Parts per Billion
PAP	Portable Air Purifier
SEM	Scanning Electric Microscope
SMPS	Scanning Mobility Particle Sizer
NaCl	Sodium Chloride (Salt)
3D filter	Three-Dimensional Filter
TVOC	Total Volatile Organic Compounds
UFP	Ultrafine Particle
VOC	Volatile Organic Compounds
V	Volume

1. Introduction

The current thesis expresses the possibilities of removing UFPs from indoor air, and the limitations and the applications of existing air cleaning technologies. In this chapter, the properties of pollutants including UFPs, their health effects and the existing methods to remove them from indoor air will be presented briefly. In addition, the fundamentals of fluid dynamics and the principles of air flow patterns in the room will be presented. At the end, the scope of the work and the limitations occurring in the current study will be addressed.

1.1. Pollutants in indoor air

Numerous air pollutants including gasses and particles exist in indoor air. The particles are divided into coarse, fine and ultrafine according to their diameters (Harrison, 1999). As shown in Figure 1.1, the term of ultrafine particle (UFP) is applied for the particles with aerodynamic diameters smaller than 100 nm (Preining, 1998) which represent the highest number as compared with fine and coarse particles (Kittelson, 1998). Ultrafine particles typically originate from combustion processes or condensation of gases with low volatility (Seinfeld and Pandis, 1997). The concentrations of UFPs indoors are influenced by indoor activities, e.g., cooking and candle burning and outdoor sources, e.g., traffic (Afshari et al., 2005).

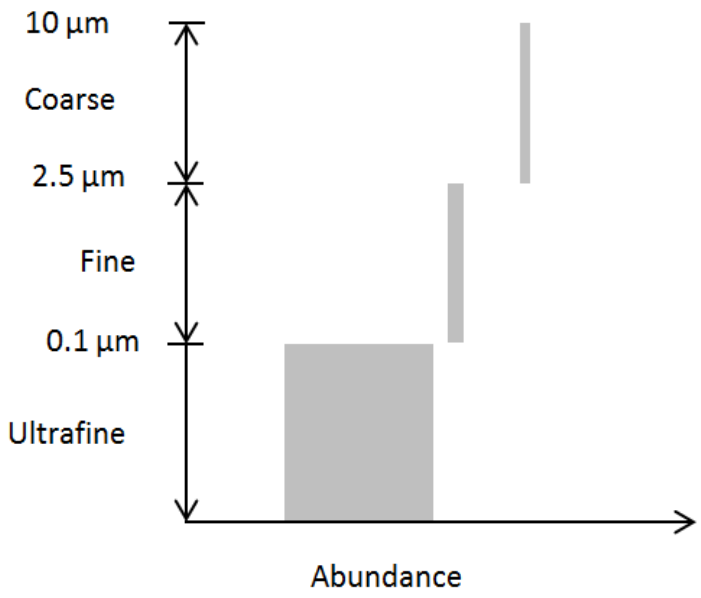

Figure 1.1 Schematic view of the size range of Ultrafine, fine and coarse particles and their abundance

Every single particle has its own shape, chemical composition, volume, weight etc. The movements of particles depend on electrical forces, inertial forces, diffusion and convection. Turbulent diffusion is an important factor in the transport of UFPs in the air, while for large particles the main factors are inertial force and gravitational force.

UFPs have negative health effects on the functions of human body organs including cardio and lungs (Bräuner et al., 2007; Anderson et al., 2010; Bräuner et al., 2008; Knol et al., 2009; Utell and Frampton, 2000). Particles in the UFP size range are not captured in the upper nasal tracts due to their size, and they can settle deep down in the lungs (Ibald-Mulli et al., 2002; Penttinen et al., 2001).

Some gasses including, among others, carbon monoxide (CO), volatile organic compounds (VOC) and ozone are considered as pollutants. Exposure to concentrations of ozone higher than 120 μgm^{-3} has a hazardous effect on living organisms ("Air Quality Guidelines for Europe", 2000; Zwick et al., 1991). Ozone is a gas whose toxicity has been studied broadly (Menzel, 1984; Neidell, 2009). In addition, ozone reacts with terpene and other unsaturated organic compounds (Fan et al., 2003; Weschler and Shields, 1999). These reactions will result in the generation of new UFPs, which are called secondary aerosols (Rohr et al., 2003; Singer et al., 2006).

1.2. Improving the indoor air quality

There are three main methods of improving the indoor air quality regarding UFPs: removing the pollutant source, dilution by supplying air from outside by a ventilation system and cleaning the indoor air with an air cleaning technology. The aim of a ventilation system is to fulfill human needs for a healthy and comfortable indoor climate. The aim may be reached by removing excess heat and pollutants from the air and supplying fresh air to the room.

In order to remove a pollutant, source control should always be the first method applied. When source control is not possible or practical, using a ventilation system should be the next option. But in current urban environments, the outside air itself is one of the main sources of pollution. Therefore, when it is obvious that neither of the first two methods would reduce the level of the pollutant in the space, an air cleaning method should be applied.

Indoor climate is an important issue and the quality of supplied air and space-conditioning must improve and become more energy efficient. In order to meet the future challenges of the building energy demand, the objectives of this study was to improve indoor air quality while energy saving was justified.

The aim of using a portable (in-room) air cleaner is in line with these aims. However, a portable air cleaner is not a substitute for ventilation. Different air cleaning technologies have been introduced to the market. Non Thermal Plasma, Corona Discharge Ionization, mechanical filters including High Efficiency Particulate Air (HEPA) filters, and electrostatic fibrous filter technologies are among the technologies used as air cleaners.

There are two main concepts for cleaning the air: mechanical and chemical. Mechanical air cleaning is accomplished with different filters such as HEPA filters. Adding filter to a duct causes a pressure drop and consequently increases the energy consumption of the ventilation system.

1.3. Simulation of an indoor airflow pattern by CFD

It has been for decades that CFD simulation has been used to study fluid dynamics. This method of study is rather new in compared with experimental studies and consequently, the procedure of the CFD simulation is not settled for all case studies (Baker et al., 1994). A simulation can reduce needs for expensive tests and consequently reduce the cost of a project.

Computational methodology of simulation includes

1- Specifying the boundary condition of the fluid domain

2- Specifying the physical characteristics of the flow

3- Selecting numerical approaches and algorithms

4- Specifying initial conditions

5- Discretizing the geometry

6- Solving iteratively the discretized form of governing equations for the discretized domain

7- Evaluating the results in comparison with the experimental data

If the prerequisites of this method have been addressed, the CFD method can determine computationally the flow properties of interest. However, some procedures are needed in order to validate a CFD solution. Two main procedures are checking the grid-independency of the solution and experimental validation of the results. Grid-independency means that it is essential to ensure that the solution is independent of the size of the meshes used to discretize the domain. Experimental validation is needed in order to certify if the CFD solution is physically correct.

Mainly, there are two approaches for simulating the dynamics of pollutants including particles: the Eulerian approach and the Lagrangian approach.

The Eulerian approach assumes that the behaviour of the particle phase is similar to the continuum, while the Lagrangian approach considers the particles as single points (Crowe, 2005). Studies have been conducted on the particle phase models combined with different turbulence models for different particle sizes (Wang et al., 2012). In most studies, the simulated particle sizes are in the range of fine particles or coarse particles, i.e. particles larger than 100 nm.
CFD simulation has been used to study the air cleaners inside a room, and to evaluate different initial conditions and turbulence models (Zhang et al., 2010). In addition, the impact of the placement of air cleaners has been studied (Zhou et al., 2009).

1.4. Hypothesis

This study intends to illustrate the potential for saving energy and at the same time to utilize the technical installations for providing treated good quality air for occupants. The main hypothesis of this study is that it is possible to recirculate air inside a room and reduce the amount of supply air while the indoor air quality is kept at an acceptable level. According to the current rules of Danish building regulation, it is not allowed to reduce the supply air and instead have recirculation of air in the building.

The hypothesis is also that it is possible to improve the indoor air quality when the facts behind the dispersion of UFPs in an indoor environment are known.

1.5. Scope

The scope of this study is to investigate limitations, possibilities and applications of using recirculated air in combination with new air cleaning technologies in order to improve indoor air quality. The objective of this study is to determine the effectiveness of portable air cleaners and to investigate the approaches of using these devices aiming at reducing the concentration of UFPs in the indoor environment.

1.6. Methods and limitations

This study concentrated on the particle removal abilities of different air cleaning technologies. The experiments included measurements in a duct, a clean room and an office room. The measuring devices that were used to measure UFPs and gasses had some systematic errors and limitations. In the experiments, five air cleaning technologies were selected among different technologies in the market.

In order to study the dispersion of UFPs in the room, CFD software was used. The computational solution method is an approach to achieve the solution which has some deviations with the exact solution. The particle phase was simulated by mainly using the Lagrangian approach, while there are other approaches that were not applied in this study.

2. Experimental investigations

This chapter describes experimental investigations performed on the air cleaning technologies. The chapter will start with a background description regarding UFPs and air cleaning technologies. The chapter will continue with the methods that were used, and finally some parts of the results will be presented.

2.1. Background

The adverse health effects of particles on humans have been studied and it has been well established that particles including UFPs have adverse health effects on the human body (Bräuner et al., 2007; Anderson et al., 2010; Kappos et al., 2004; Song et al., 2011; Strak et al., 2012; Utell and Frampton, 2000).

Particles deposit on different places of a lung depending mainly on their sizes (Brown and Cook, 1950). Figure 2.1 shows three regions in the respiratory tracts where particles deposit by three mechanisms: Inertial impaction, sedimentation (interception) and diffusion. UFPs can lodge deep into the respiratory tract to the pulmonary alveoli, since they are not stopped by inertial impaction and interception. UFPs have a high alveolar deposition fraction because of large surface area compared with their mass, chemical composition, and ability to translocate (Ibald-Mulli et al., 2002; Penttinen et al., 2001).

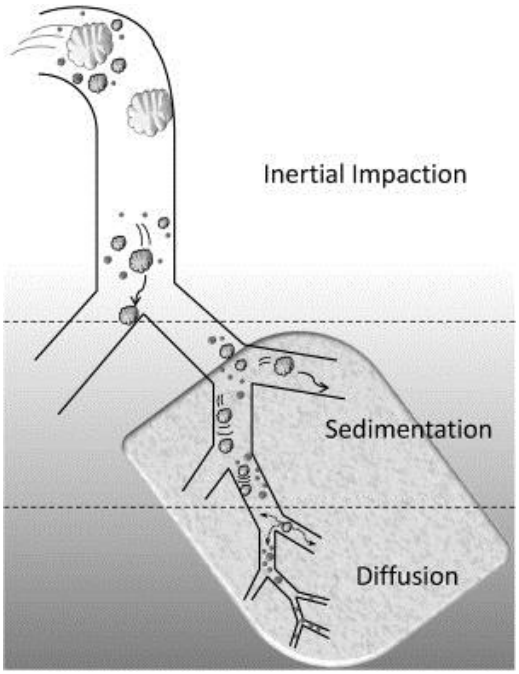

Figure 2.1 Three regions of the respiratory tracts and their deposition mechanisms (Carvalho et al., 2011)

In addition, the number of UFPs in urban ambient air is high compared with rural ambient air, and the sources of UFPs in outdoor air are a variety of urban/industrial processes. A study in Copenhagen shows that the concentration of UFPs is the highest among the particle fractions (Bräuner et al., 2007).

Different technologies have been invented to be used as an air cleaner, including mechanical filters, plasma technology, ozone-initiating technology, electrostatic precipitation, photocatalytic oxidation and technologies using O_3, Tio_2 and UV (Destaillats et al., 2011; Zhang et al., 2011).

Ozone initiating air cleaning technologies have been assessed with regard to the rate of the ozone that they generate, maximum ozone level in a room, particle generation and the health effects of ozone. Some methodologies are introduced to predict the maximum ozone level caused by an air cleaner using the background level, the initial slope of the ozone growth curve and other factors (Niu, 2001; Tung, 2005).

In order to determine the capability of an air cleaner in removing pollutants, researchers have introduced the term ‘effective cleaning rate’, which was later replaced by the term ‘clean air delivery rate’ (CADR). CADR is the difference in the detected pollutant decay rates with and without the air cleaner multiplied by the room volume (Shaughnessy and Sextro, 2006). In other words, the decay rate of a pollutant is determined first in a room without any air cleaner in operation. Then the decay rate is determined for the room with an air cleaner in operation. The difference between the decay rates is caused by the air cleaner. The difference multiplied by the room volume will result in CADR.

Nazaroff (2000) has determined effectiveness as a new property in order to evaluate the influence of an air cleaner on the indoor pollutant concentration. This effectiveness shows how an air cleaner is effective for a room with a specific air change rate. Researchers have used this definition and

determined the effectiveness of different air cleaners (Grabarczyk, 2001; Sublett, 2011; Zhang et al., 2010).

It is common for manufacturers of air cleaners to claim that their technologies can remove pollutants effectively. However, some studies have revealed that the manufacturers' claims are not valid, and some of the technologies themselves can cause the generation of particles (Alshawa et al., 2007; Hubbard et al., 2005; Waring et al., 2008).

In addition to the investigation of the ozone initiating cleaning technologies, this study focuses on fibrous filters. A fibrous filter is a filter comprising a huge number of small woven fibers ranging from Nano-size fibers to micro-size fibers. The filters and their characteristics have been studied in detail regarding pressure drop, penetration ratio, filter efficiency (Brown, 1993; Japuntich et al., 1994). Figure 2.2 shows a microscopic view of a fibrous filter.

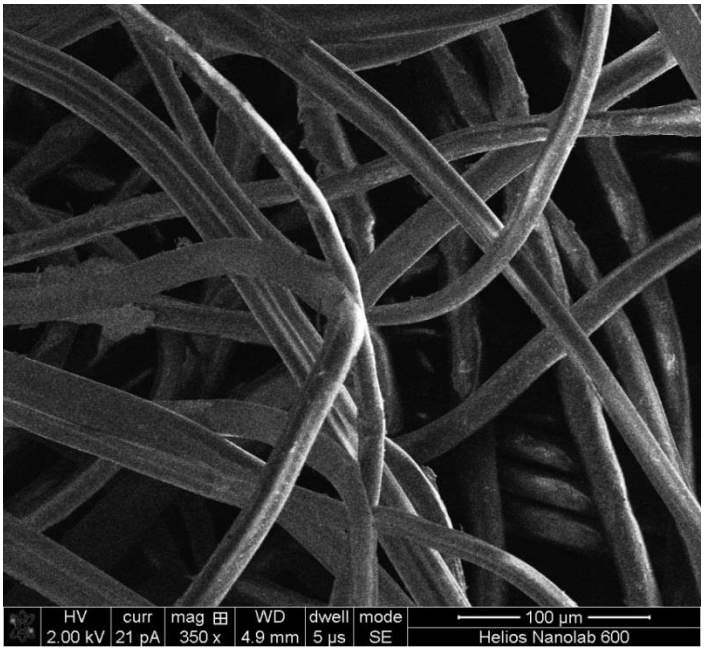

Figure 2.2 Microscopic view of an electrostatic fibrous filter

The particles are captured by the filters by means of diffusion, interception, impaction, electrostatic charge and gravitational settling. The influence of the mechanisms depends on the size of the particles. The minimum efficiency of a filter has been reported for particles with diameters between about 100 nm to about 300 nm, for which the effects of particle removal are the lowest for diffusion and impaction mechanisms. Moreover, the effect of air velocity on the filter removal efficiency in capturing UFPs has been tested. The removal efficiency decreases with increasing velocity (Brown, 1993; Stafford and Ettinger, 1972).

According to studies performed to assess the filter charge effect on the efficiency of the filter in removing particles, the size-fractional efficiency of the charged filters for particles ranging from 10 nm to 10 µm are higher than in a normal glass fiber filter. In addition, the efficiency of the charged filters reduces gradually over time (Baumgartner et al., 1986; Baumgartner and Löffler, 1986).

2.2. Methodologies

The methodology of the experiment part included the following steps:

a. Literature reviews regarding particles, measuring devices and air cleaning technologies
b. Searching the Danish market for the newest air cleaning technologies
c. Learning experimental procedures
d. Calibrating instruments
e. Conducting the experimental investigations according to accepted models.
f. Evaluating the results and discussing the hypothesis

The outcome of the first steps, i.e. literature review, is summarized in the Background section. In the following sub-sections, other steps will be explained.

2.2.1. Particle counters

Different technologies have been introduced for counting the number concentration of particles including UFPs. In this study, three particle counters were used in order to measure number concentrations comprising NanoTracer, Scanning Mobility Particle Sizer (SMPS) and Condensation Particle Counter (CPC).

An electrical aerosol detector applies electrical charge to count the number of particles. It introduces a specific electrical charge to the particles and later counts them according to the electrical mobility of the particles. NanoTracer PNT1000 is an electrical aerosol detector that can detect the total number of particles ranging between 10 and 300 nm with a concentration range of 0-10^6 UFPs/cm^3.

Another technology is the Condensation Particle Counter (CPC) which uses Butanol or water for counting particles. The liquid is converted to saturated gas, which condenses on the surface of the particles and forms the liquid droplets. The condensed drops can be counted using the light-scattering method. The instrument, CPC 3007, can count UFPs between 10 nm and 1 micrometer (µm) with a concentration range of 0-10^5 UFPs/cm^3.

Scanning Mobility Particle Sizer (SMPS) is a technology that classifies the particles according to their sizes by electrical charge and later counts the number of each size by means of the method of condensation particle counter. In the present study, the SMPS which was used in the experiments was set to count particles with a diameter range of 7- 298 nm.

2.2.2. Measuring instruments

The ozone level was logged by the ozone monitor *BMT 930* and the ozone monitor *2B Technologies* model 205. The ozone monitors was able to detect the ozone level down to 1 ppb accurately. The gas monitors *Brüel&Kjær*, model 1302 and Innova model 1312, were used to measure TVOCs during measurements. The detection limit of the gas monitors typically is 1 ppb; however it can change depending on the gas which is being monitored. *Tinytag Ultra* temperature loggers were used to measure the temperature and the humidity during the measurements. The velocity was measured by means of a *Dantec* anemometer. In order to determine the pressure differences, a digital monometer was used.

2.2.3. Air cleaning technologies

In order to study the air cleaning technologies, the Danish market was searched, and five air cleaning technologies were selected, including Non Thermal Plasma, Corona Discharge Ionizer, Portable Air Purifier, Electrostatic Fibrous Filter and Three Dimensional Filter. The selected technologies will be briefly introduced here.

Non-thermal Plasma technology (NTP): It is a specific kind of NTP that has two coaxial cylinders and a barrier which is located between the cylinders. Because of the high voltage difference between the cylinders, the electrons move to the lower voltage side, but because of the barrier, the electrons cannot flow to the other cylinder. Instead, the electrons discharge into the air and cause reactions. As shown in Figure 2.3, the air flows through the discharge gap between glass tube and outer cylinder, which is covered by a cooled steel tube, and reactions including generation of ozone occur.

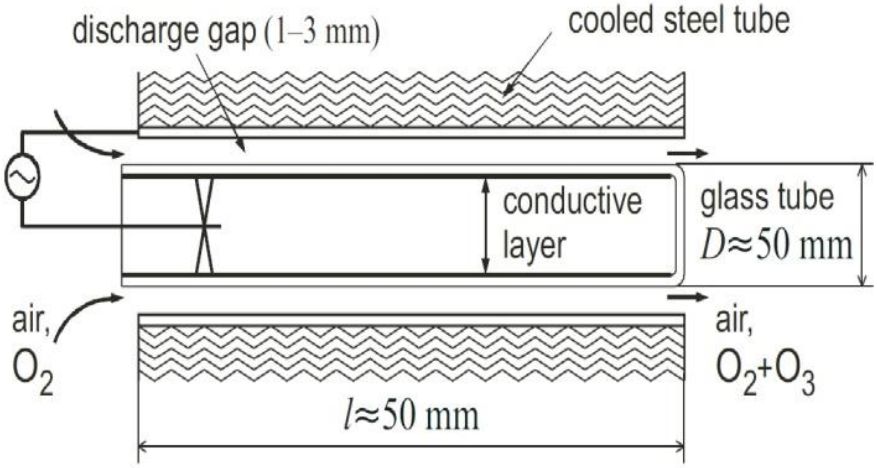

Figure 2.3 Schematic view of the Non-thermal Plasma technology (Pekárek, 2003)

Corona Discharge Ionizer (CDI): The schematic picture of this technology is shown in Figure 2.4. The performing principle of this technology is similar to NTP, i.e. discharge of the electrons to the air. However, it has a needle and a plate to discharge particles. The corona of electrons is produced using high voltage electricity, and the electrons are injected from the needle to the air passing between the plates (Paper I).

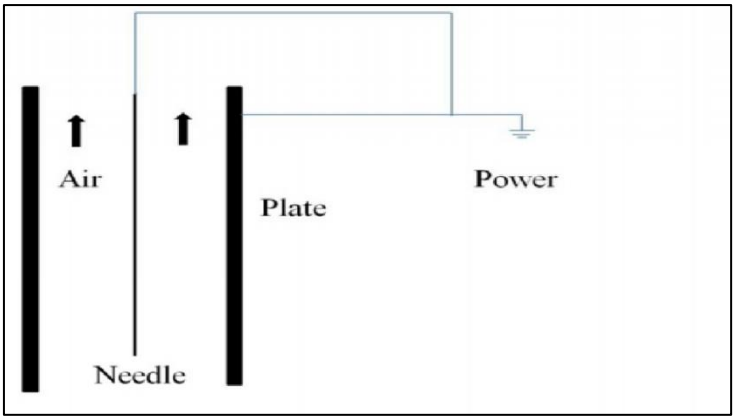

Figure 2.4 Schematic view of the Corona Discharge Ionizer technology

Portable Air Purifier (PAP): This is a novel technology comprising UV light, ozone generator, electrostatic precipitator and ozone filter. It simulates the reactions of the atmosphere at the level of the stratosphere, which is a layer of the earth's atmosphere starting from 12 kilometres above the earth. As shown in Figure 2.5, the ozone molecules are generated by an ozone generator. The UV lights installed in the interior wall of the air cleaner excite the generated ozone molecules, and the excited molecules react with contaminants in the air and generate oxidised substances (Paper I).

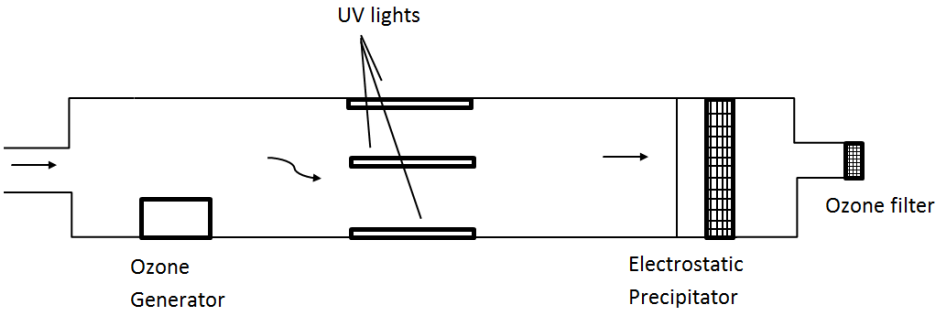

Figure 2.5 Schematic view of the Portable Air Purifier technology

This oxidation process causes the particles to grow in size, and finally they are captured in an electrostatic precipitator. An ozone filter is used at the end of the process to remove the ozone from the air.

Electrostatic Fibrous Filters (EFF): A fibrous filter with electrostatically charged fibres is also selected as one of the air cleaning technologies. The packing density of the filter is 80 g/m^2 and the size of the fibres of the filter is between 10 and 20 µm. Different types of electrostatic fibrous filters are used to clean the air in ventilation systems. The fibres of a filter are charged electrostatically to improve the cleaning ability of the filter. In the remaining part of this thesis, this technology will be called EFF.

Three-dimensional filter (3D Filter): The last air cleaning technology was a filter with electrostatically charged fibres, similar to the fibres of the EFF technology. However, the fibres of this filter are packed differently. One side of the fibres is attached to a grid. Thousands of fibres are attached to a grid inside a frame. The air can pass along the fibres through the gap between the fibres.

2.2.4. Experimental investigations in a duct

The experimental investigations in a duct were performed in order to evaluate the efficiency of the air cleaners according to ANSI/ASHRAE Standard 52.2-2007. The air cleaners were also placed in a duct and connected to a clean room in order to identify and quantify the eventual airborne pollutants generated by them. First, the measurements were carried out when the air cleaners were

in operation individually and the particle source was not active. The aim was to assess the efficiencies of the air cleaners.

The measurements continued to evaluate the efficiency of the technologies. The UFPs were generated by one pure wax candle in the room. The candle was burnt until the steady state concentration was reached. The air inside the room was well mixed by means of two small fans. After reaching the steady state particle concentration in the room, the concentrations of UFPs upstream and downstream of the filter were recorded. The efficiencies were calculated using Equation 2.1.

$$Eff = \frac{C_{upstream} - C_{downstream}}{C_{upstream}} \quad (2.1)$$

Here $C_{upstream}$ (UFP/cm^3) is the concentration of UFPs upstream of the flow and $C_{downstream}$ (UFP/cm^3) is the concentration of UFPs downstream of the flow.

2.2.5. Experimental investigations in a clean room and in an office room

The experimental investigations in a clean room were performed in order to evaluate the performance of air cleaners under controlled conditions according to standard ANSI/AHAM AC-1-2006. Measurements were carried out to evaluate the performance of the air cleaners in a clean room and in an office room. The same procedures were used for experiments in the office room. The clean room had walls that were made of glass and steel. The air supplied to the clean room was cleaned by a charcoal filter and a HEPA filter. The volume of the clean room was 30 m^3 with a floor area of 10 m^2. The office room was an unoccupied room with the volume of 47.5 m^3, located in an empty building. The office room had not been renovated for two decades, and therefore the building materials were old.

In the first step, each air cleaner was in operation individually in each room to evaluate its performance and byproducts. Then a candle was used to evaluate the effectiveness of the air cleaning technologies in removing UFPs.

The UFP concentration, ozone and total volatile compounds (TVOC) were monitored during all of the measurements. The background concentration of UFPs was less than 500 (UFP/cm^3) inside the clean room. The particle counters logged the data in the middle of the room at a height of 1 m. The air cleaners were in operation individually without any pollution source in the room during the first step. This step of the experiments was performed for PAP both in summer and winter.

In the second step, the effectiveness of the air cleaners was evaluated with a particle source in the clean room and in the office room. This method is called in situ method (Offermann et al., 1985). The procedure of the method is that a contaminant is added to a room, and the air is mixed, using small fans. After achieving the steady state condition regarding the concentration of the contaminant, the contaminant source is removed and the concentration of the contaminant continuously logged. The decay rates for the cases without an air cleaner and with an air cleaner are calculated using the logged data. In this study, a candle was burnt in the room and the air was well mixed by two small fans. The air change rates of the rooms were measured by the tracer gas N_2O.

At the first segment of determining the effectiveness, the air cleaner was off and the particles were removed by the ventilation system and deposition. At the second segment, the candle burnt again and after reaching the steady state condition, the air cleaner was turned on. The particles generated

by the candle were removed with the air cleaning technology together with the ventilation system and deposition. The particle removal rate caused by the air cleaning technology is obtained using Equation 2.2.

$$\lambda_{AC} = \lambda_{(AC+v+d)} - \lambda_{(v+d)} \quad (2.2)$$

Where $\lambda_{(AC+v+d)}$ (h^{-1}) is the removal rate when the air cleaner is on, $\lambda_{(v+d)}$ (h^{-1}) is the removal rate when the air cleaner is off, and λ_{AC} (h^{-1}) is the removal rate caused by the air cleaner.

The Clean Air Delivery Rate (CADR) is the removal rate caused by the air cleaner (λ_{AC}) which is the difference in the detected particle decay rates with and without the air cleaner in operation, multiplied by the room volume and calculated by Equation 2.3 (Shaughnessy and Sextro, 2006).

$$CADR = V_R \times (\lambda_{AC}) \quad (2.3)$$

Here V_R (m^3) is the volume of the room.

The effectiveness of an air cleaner provides more information than CADR (m^3/h) regarding the ability of an air cleaning technology in removing pollutants from the indoor air of a room. The air cleaner effectiveness is calculated using the following equation.

$$\varepsilon = \frac{CADR/[V(\lambda_{(v+d)})]}{1+CADR/[V(\lambda_{(v+d)})]} \quad (2.4)$$

In fact effectiveness is the ability of an air cleaner in reducing a specific pollutant such as UFP. If the pollutant concentration in a room is C_{ref} (UFP/cm^3) and after adding an air cleaner the concentration in the room is reduced to the new concentration C_{ctrl} (UFP/cm^3), the effectiveness can be determined by the following equation:

$$\varepsilon = \frac{C_{ref}-C_{ctrl}}{C_{ref}} \quad (2.5)$$

The effectiveness is directly and closely related to the key outcome of interest: how much does the use of this cleaning technology improve indoor air quality.

2.2.6. Studying filtration dependency on ultrafine particle exposure and composition

More investigations were performed on EFF technology regarding the dependence of the filter's efficiency on particle exposure and composition. The measurement was set up according to Figure 2.6 in order to evaluate its efficiency at different levels of UFPs. The tests were performed at five levels of UFP concentrations, ranging from approx. 2,800 UFP/cm^3 to 100,000 UFP/cm^3. The filter was tested at the flow rates of 60 l/s and 100 l/s. During all of the measurements, the UFP concentration was measured by means of NanoTracer PNT 1000 and SMPS upstream and downstream of the filter simultaneously.

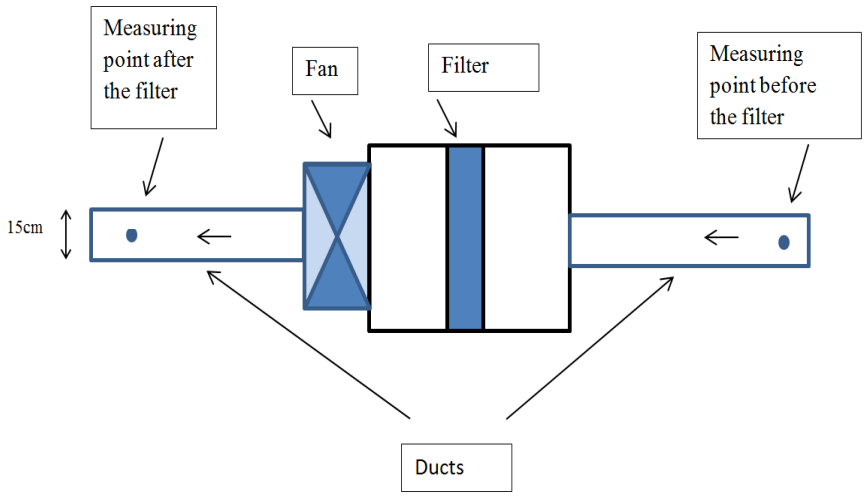

Figure 2.6 The filter was placed in a steel box and connected to the test room

The pressure difference was measured before and after the filter by a digital manometer. In addition, an optical microscope and a Scanning Electric Microscope (SEM) were also used to study the dendrites of the UFPs formed on the fibres. According to the microscopic visualizations by SEM, the sizes of the fibres of the filter were between 15 µm and 20 µm.

The filter was also examined regarding the resuspension of the particles. The filter was placed in a box, and through a duct it was connected to the test room, where high concentrations of particles were generated by a candle. A fan was placed along the duct to cause the flow rate of 60 l/s through the filter. The filter was loaded for 1 hour. The fan was stopped, and the ducts were blocked to prevent the air flow through the filter. Then the setup of the filter in the box was connected to the clean room through a duct, and the clean air passed through the filter to study the resuspension of the filter.

2.2.7. Electrostatic fibrous filter technology combined with a chilled beam

The EFF was also combined with a chilled beam to study the particle removal ability of the EFF when it is combined with a chilled beam. The chilled beam is used to supply fresh air to a room while the excess heat generated in the room is also extracted. A schematic view of the combined system is shown in Figure 2.7. The primary airflow came from the supply duct as shown by No. 1 in the figure. The induced secondary airflow (No. 2) passed through a mechanical filter (No. 3) located below a water coil (No. 4). The excess heat of the induced secondary air is given off to the water in the coil and returned to the room together with primary air because of the entrainment effect (Paper IV).

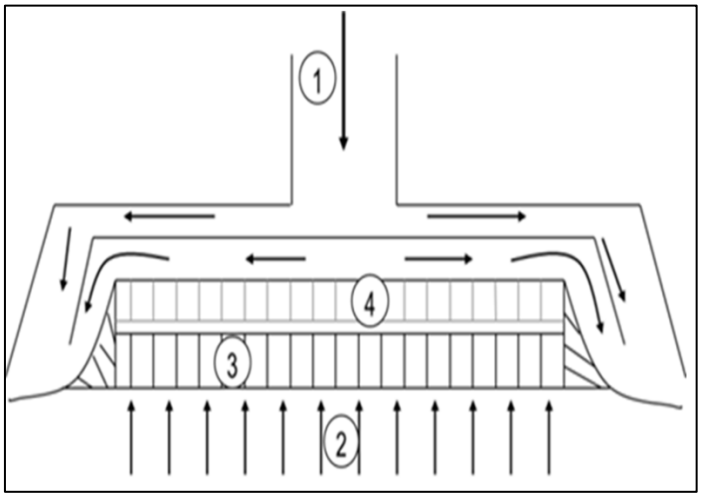

Figure 2.7 Schematic view of a combined system (Paper IV)

The sensible heat removal effect of a chilled beam refers to the amount of energy that can be extracted from the air by a chilled beam per time unit. This is determined by Equation 2.6.

$$H=f\times C\times \Delta T \tag{2.6}$$

Where H (W) is the effect, f (kg/s) is the water flow rate, C ($Jkg^{-1}K^{-1}$) is the specific heat capacity of water and ΔT (K) is the temperature difference between supply water and return water.

The experiments of the combined system were performed in a laboratory room with a volume of 51 m^3. The combined system was located in the middle of the ceiling in order to conform to the location best suited for a chilled beam (Loudermilk 2009).

Two sources of particles were used to measure the effectiveness of the filter in removing organic and inorganic material. The pure wax candle was chosen, since wax is an organic material that is not soluble in water. The other material was salt (NaCl) as it is an inorganic material that is soluble in water, and therefore static charge is hard to be build up on its surface. The particles were generated first with a pure wax candle and then with an aspirator to generate aqueous-based salt particles. The UFP source was located on the floor in the middle of the room.

2.3. Results

2.3.1. Comparing the particle counters

The three particle counters which were evaluated in this PhD study were NanoTracer, SMPS and CPC. At a low level of UFPs, the results of the three counters were similar. As shown in Figure 2.8, NanoTracer showed more fluctions in UFP concentrations below 2000 UFPs/cm^3.

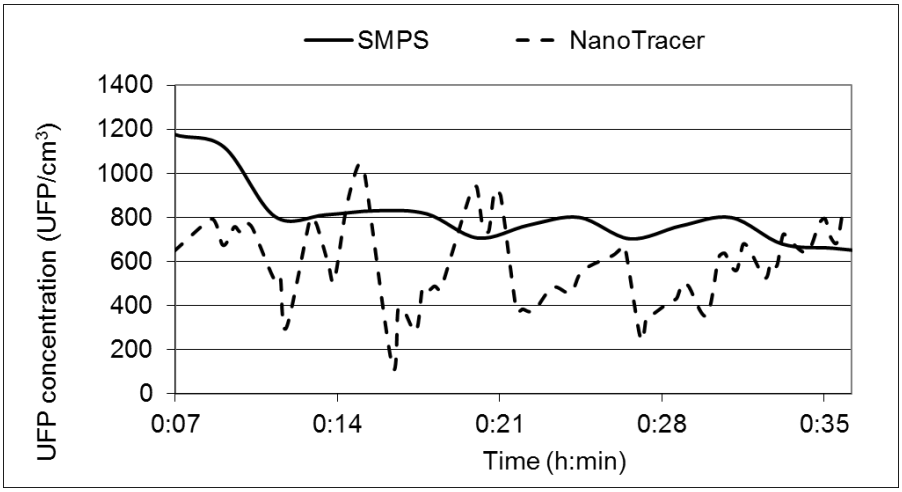

Figure 2.8 Comparison of registered data of the NanoTracer with SMPS for the concentration of UFPs (less than 2000 UFPs/cm^3)

With the concentration higher than 90,000 UFPs/cm^3, logged data of the NanoTracer and the SMPS were related by an exponential equation, while CPC did not show any change.

2.3.2. Experimental investigations on the air cleaners in a duct

First, the air cleaners were evaluated in the duct without any particle source. In this part of the study, there was no particle source in the test room. The results show that the level of ozone increased by 44%, 33% and 11% for NTP, CDI and PAP respectively. Two other technologies, namely EFF and 3D Filter, are mechanical filters, therefore they do not generate by-products.

The second step of the duct experiment was to determine the efficiency of the air cleaning technologies in removing UFPs generated by a pure wax candle. The candle was burnt in the clean room and the air cleaner was connected to the room by a duct. The result is shown in Table 2.1.

Table 2.1 Efficiency of the air cleaning technologies in removing UFPs (Paper I)

Air cleaners	Efficiency
NTP	9%
CDI	40%
PAP	15%
EFF	78%
3D Filter	50%

2.3.3. Experimental investigations on the air cleaners in a clean room

In the second part, air cleaners were in operation in a clean room. The first step was to investigate the substances that could be created by the technologies when they worked alone in the clean room. Table 2.2 shows the maximum UFP concentration and maximum ozone concentration in the clean

room for the experiments of the three technologies. The two other technologies, i.e. EFF and 3D Filter, did not generate ozone nor UFPs.

Table 2.2 Concentration of UFP and ozone for air cleaners in the clean room (Paper I)

Air cleaners	Summer		Winter	
	Ozone (ppb)	UFP (UFP/cm^3)	Ozone (ppb)	UFP (UFP/cm^3)
NTP	28	20000	-	-
CDI	35	1100	-	-
PAP	8	23000	8	5000

The technologies PAP and NTP caused an increase in the UFP concentration in the room while CDI did not cause a change.

The particle concentration started increasing after a delay of about one hour. As shown in Figure 2.9, after about two hours, the concentration reached its ultimate level, and then the concentration started falling.

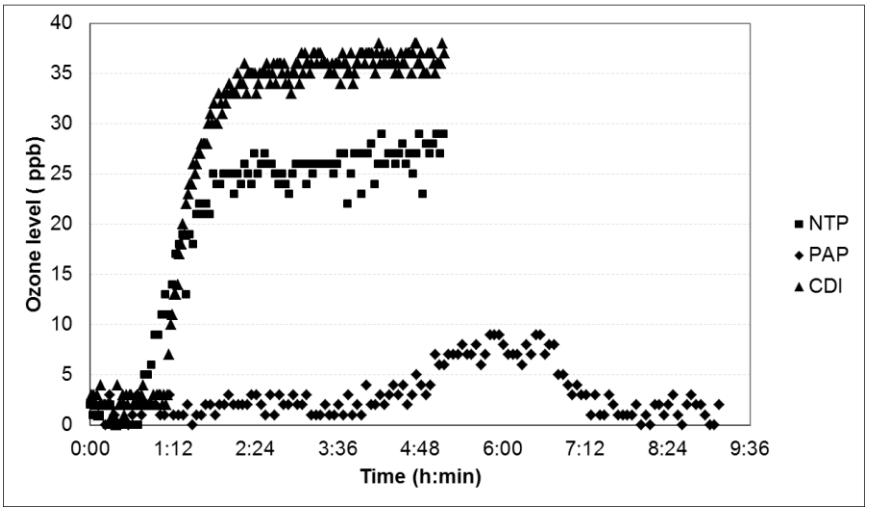

Figure 2.9 Concentration of ozone of the room with air cleaners NTP, PAP and CDI

In the second step of the clean room experiments, the effectiveness of the air cleaners in removing UFPs was evaluated. Table 2.3 shows the CADR and effectiveness of the air cleaning technologies in removing UFPs. The second column in the table displays the UFP removal rate of the ventilation system together with an air cleaner. The third column is associated with the UFP removal rate caused by the ventilation system and deposition. The CADR and the Effectiveness, which are shown in the fourth and fifth columns, are calculated according to Equation 2.3 and Equation 2.4. As is shown in the table, the highest CADR and effectiveness belong to the EFF technology.

Table 2.3 Effectiveness of the air cleaners in removing UFPs generated by a candle inside a clean room (Paper I)

Air cleaners	UFP removal rate of system with air cleaner ($\lambda_{ac}+\lambda_v+\lambda_d$)	UFP removal rate of system without air cleaner ($\lambda_v+\lambda_d$)	CADR (m^3/h)	Effectiveness (ε)
NTP	3.5	2.8	20	0.2
CDI	4.3	2.7	50	0.4
PAP	3.4	2.8	18	0.2
EFF	9.2	2.5	200	0.7
3D Filter	3.4	1.7	50	0.5

2.3.4. Experimental investigations on the air cleaners in an office room

The three air cleaning technologies, NTP, CDI and PAP increased the level of ozone in the office room.

Despite the results of the clean room experiments, the three first air cleaning technologies did not increase the particle concentration in the office room (Paper III).

In addition, the effectiveness of the air cleaning technologies in the office room was also determined, which is reported in Table 2.4.

Table 2.4 Effectiveness of the air cleaners in removing UFPs from the air of the office room (Paper III)

Air cleaners	UFP decay rate of system with air cleaner ($\lambda_v+\lambda_d$)	UFP decay rate of system without air cleaner (λ_{ac})	CADR (m^3/h)	Effectiveness (ε)
NTP	1.1	0.9	13	0.2
CDI	3.6	1.2	110	0.4
PAP	1.3	0.9	20	0.25
EFF	5.2	1.4	180	0.42
3D Filter	3.7	1.2	110	0.4

2.3.5. Studying filtration dependency on ultrafine exposure and composition

More evaluations were performed on EFF technology in a duct. The evaluations comprised two parts. First, different UFP concentrations were generated using a candle, and after achieving a steady state condition, the particle concentrations both before and after the filter were logged. The

fractional efficiency (efficiency for particles of a size) of the filter is shown in Figure 2.10 for two different concentrations, low concentration and high concentration. When the size of the particles increases, the efficiency decreases as shown in the figure.

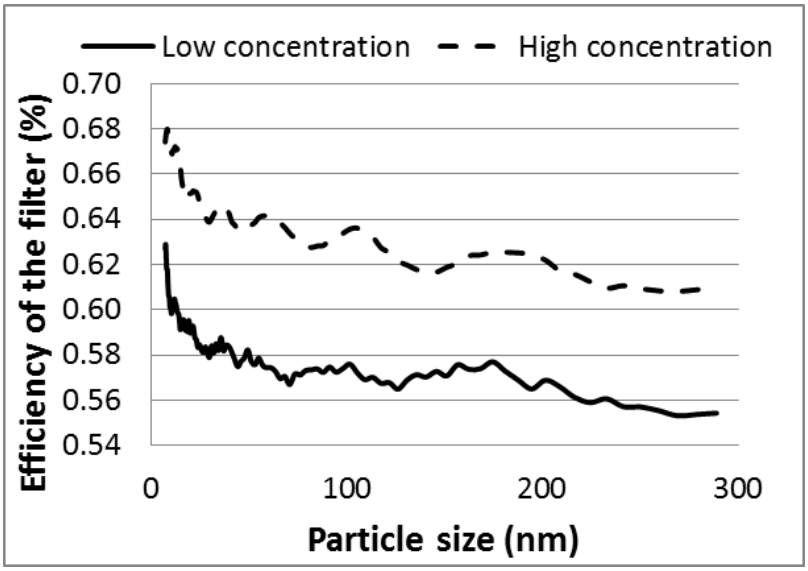

Figure 2.10 Efficiency of the filter for different sizes of the particles in two concentrations (Paper VII)

In the second part of the measurements, the candle was extinguished and the particles were removed by ventilation systems and filter. The decay rates of the particles with a diameter of 7 nm (which is the smallest size of particles counted) measured before and after are shown in Figure 2.11.

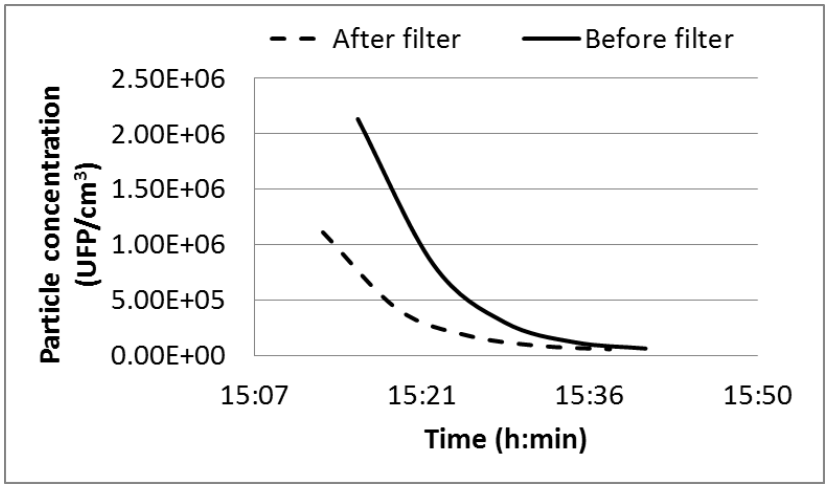

Figure 2.11 Decay rate of number of particles with diameter of 7 nm before and after the filter (Paper VII)

The efficiency of the filter was also calculated using the data logged by NanoTracer. NanoTracer shows one number at a time as the total UFP concentration. Therefore, efficiency can be calculated

according to the total UFP concentrations shown before and after the filter. The result is shown in Figure 2.12.

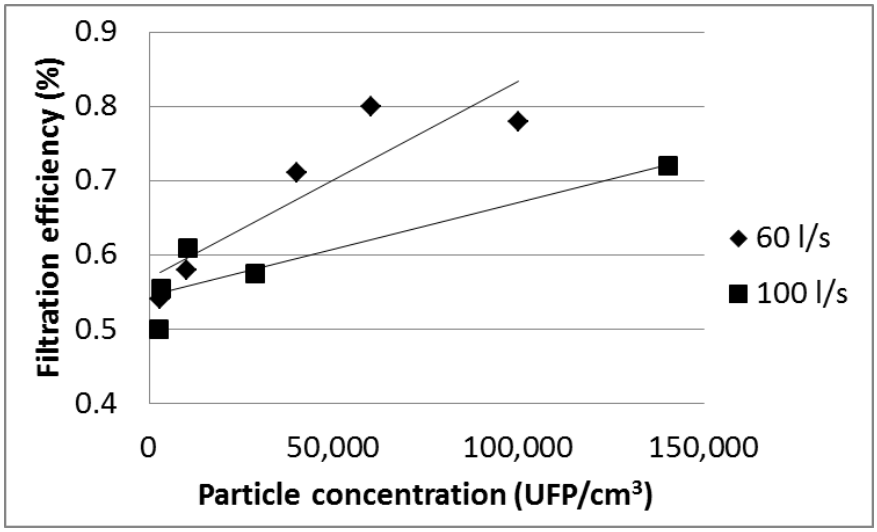

Figure 2.12 Efficiency of the filter for different sizes of the particles in flow rates of 60 l/s and 100 l/s

The efficiency measurement was repeated with salt particles generated with the atomizer. The result is shown in Table 2.5.

Table 2.5 Efficiency of the filter in two concentrations of salt particles

Test No.	UFP concentration upstream (UFPs/cm^3)	Efficiency (%)
1	72000	41
2	63000	38
3	34000	42

2.3.6. EFF technology combined with a chilled beam

The EFF is selected to be combined with a chilled beam to evaluate the improvement in particle removal rate by a chilled beam.

Figure 2.13 shows the removal rate of the particle concentration generated by a candle in a room. The candle burnt until the UFP level reached a steady state. Then the candle was extinguished. The upper line shows the removal of the UFP concentration when the chilled beam was in operation in the room without the filter. The UFP removal rate due to ventilation and deposition was estimated using the exponential trend line of the curve to be 2.7 h^{-1} with R^2 equal to 0.99.

The lower line in Figure 2.13 indicates the removal rate of the UFP concentration for the combined system. The corresponding removal rate was 4.7 h^{-1}, with R^2 equal to 0.99. By subtracting the effect of the chilled beam without filter (2.7 h^{-1}) from the effect of the combined system (4.7 h^{-1}), the effect of the filter in cleaning the air was determined to 2 h^{-1}. The average diameter of the particles generated by the candle ranged between 33 nm to 47 nm.

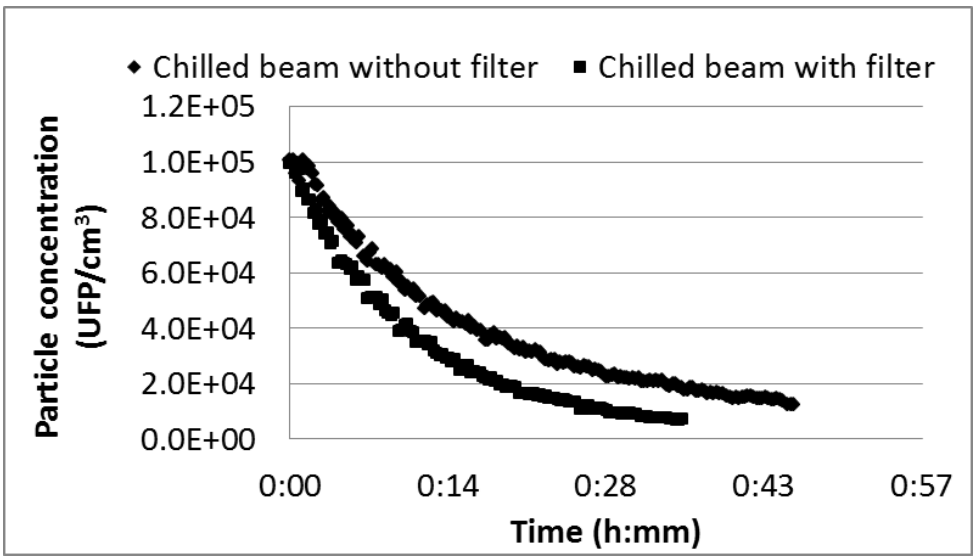

Figure 2.13 Removal of UFPs generated by a candle with a chilled beam in a room (Paper VI)

As regards the combined system, the supply water temperature was 12.3°C and the return water temperature was 14.3°C, while the return temperature was 15.3°C in the case of the chilled beam without filter with the same supply temperature. The water flow rate was 0.038 l/s. Assuming the water specific heat capacity to be 4200 $Jkg^{-1}K^{-1}$, the heat removal effect of both cases could be calculated by Equation 2.8. Consequently, it was possible to calculate the reduction of the effect caused by the filter. To evaluate the reduction, measurements were made for three primary airflows, and the result is shown in Table 2.6.

Table 2.6 The effect of three primary airflows for combined system and chilled beam (Paper VI)

Primary air flow rate (l/s)	Effect for the combined system (W)	Effect for the chilled beam (W)	Reduction in the effect (%)
15	242	390	38
25	310	435	29
45	410	525	22

3. Simulation of particle dispersion in a room

The movements of particles in the air are considered as a flow dispersed in a continuous medium. In order to study the dispersion of particles in a room, the study of the dynamics of continuous flow (as it is the carrier of the particles) and the study of the behavior of particle phase are needed.

In this chapter, the principles of air distribution in a room will be discussed. CFD will be described briefly, and the methods of particle simulation will be explained. The chapter will continue with the description of methodologies of this study, and finally the results will be reported.

The aim of this CFD study was to investigate the possibilities of improving indoor air quality regarding removal of UFPs by air cleaners. The aim was also to see the impact of the location of heat source and a passive particle source on the distribution of UFPs at different heights.

3.1. Principles of air distribution in a room

The reason of using a ventilation system is to remove excess heat and pollutants from air and supply fresh air to the room. Among others, two air flow patterns can exist in a room, mixing ventilation and displacement ventilation. Mixing air flow pattern aims to dilute polluted air by supplying fresh air of a high velocity. The high velocity of air makes high turbulence intensity. This causes a good blend and a uniform temperature at all heights of a room.

Figure 3.1 shows an example of the displacement airflow pattern. In this airflow pattern, air moves from a supply terminal located close to the floor toward the exhaust at the higher level and pushes the existing air to the exhaust. Considering the fact that there is buoyancy force with existence of a heat source, it is clear that the main direction is from bottom to top. However there are also horizontal movements in this air flow pattern due to the entrainment of the air molecules around the plume.

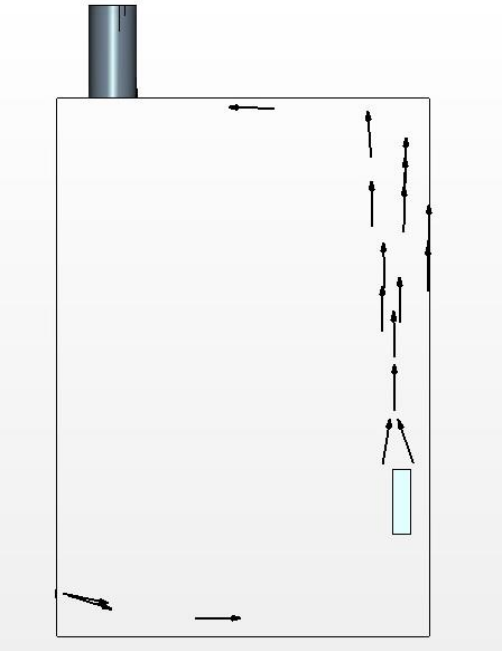

Figure 3.1 Displacement air flow pattern in a room

One of the main positive aspects of the displacement ventilation system is high effectiveness in removing excess heat from a room as it works with the principle of the buoyancy effect. In contrast, the mixing ventilation system ideally gives the same temperature for all heights.

The air with a temperature lower than the temperature of a room comes into the room through the inlet and falls down because of the higher density of cold air. Therefore, there is a temperature gradient in the room with a higher temperature at the higher part and a lower temperature at the lower part. The gradient should be restricted to avoid discomfort. As shown in Figure 3.2, there is a vertical temperature gradient. It is well-known that if the difference between the temperature at the height of a person's head and the temperature at the person's ankle become large, that person will feel draught. Draught is considered as a discomfort condition and must be avoided. Consequently, in order to keep the desired temperature gradient and remove the excess heat effectively, it is normally necessary to supply a larger amount of fresh air than that provided by the mixing ventilation system. This fact causes an increase in the cost of duct work.

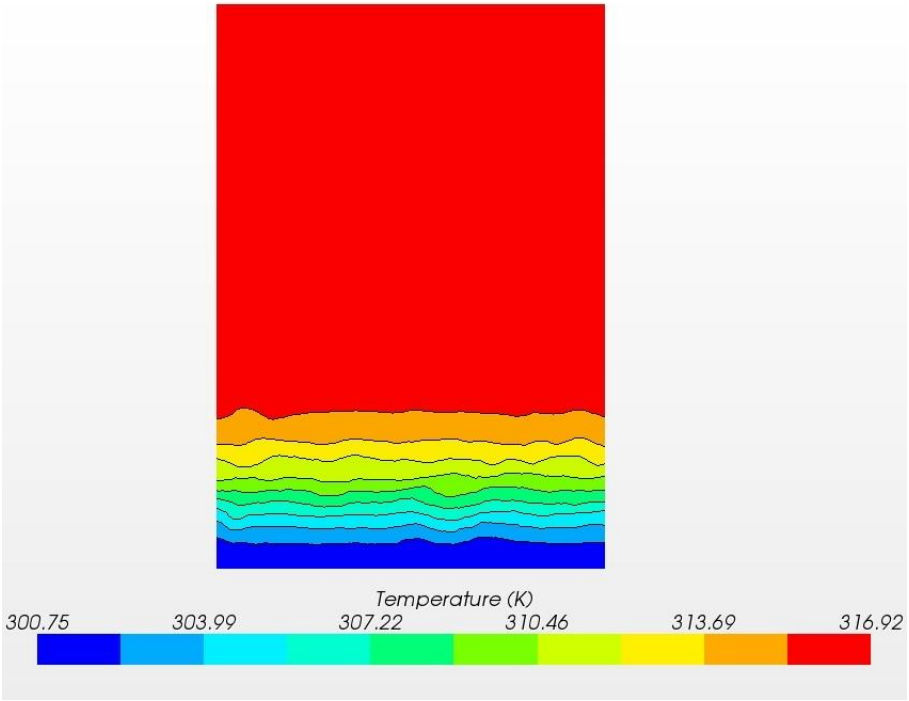

Figure 3.2 Stratification Layers in a room with a displacement airflow pattern

When using displacement ventilation, it is presumed that there is a heat source in the room. The heat source heats the air and generates plumes which move the air upward. A heat source could be occupants, a radiator, and a computer. In addition, there might be some heat sinks such as cold wall surfaces. The heat sinks reduce the temperature of adjacent air and consequently increase air density and cause down draught flows.

When the plume moves upward above a heat source, other air molecules adjacent to the plume entrain and cause an increase in the air flow rate of the plume. The plume over a heat source gets affected by the surrounding stratification. It moves upward and exchanges energy with the surroundings. It will move upward up to the height at which the temperature difference between the plume and the surrounding is zero. From this height, the plume moves upward because of inertia, then returns downward and spreads horizontally to reach the level at which the temperature difference is zero.

If a heat source has the highest heat power among all the heat sources, at a specific height, the flow rate by the air plume over the heat source minus the down draught flow rate equals the supplied flow rate. This height is called the stratification height. The height can be changed by changing the heat power of the main source and by changing the ventilation rate. There are some empirical equations for predicting the stratification height for different locations of the heat sources in a closure depending on source types (Mundt, 1996).

Jacobsen and Nielsen (1992) have evaluated displacement air distribution system in detail and have discussed the effect of boundary conditions on a displacement ventilation pattern in CFD.

Nielsen (1993) has established the important factors that must be taken into account in the design of a displacement ventilation system. The factors are free convection flows, stratification height, pollutant concentration distribution, temperature distribution and velocity distribution in the occupied zone. In addition, it has been shown that all the factors playing a role in the design of a

ventilation system can be described by an Archimedes number. In the guidebook number 1 of REHVA, displacement ventilation concept, design procedure and all other issues related to displacement ventilation have been explained (Skistad et al., 2004).

To compare the concentration profiles of pollutants in a room, a value is introduced as pollutant removal efficiency (μ) with the following equation:

$$\mu = \frac{(C_x - C_S)}{(C_E - C_S)} \tag{3.1}$$

Here, C_x (UFP/cm^3) is the concentration of the pollutant at location x, and C_S (UFP/cm^3) is the concentration of air at supply. C_E (UFP/cm^3) indicates the concentration of air at exhaust.

In order to find the adequate model to be used in a CFD simulation for a specific problem, experimental validation is recommended by experts. Detailed information regarding selection of the governing equations and the methods of evaluating results can be found in the literature sources for a specific area of research. In the simulations of a ventilation system, information regarding boundary condition estimations, turbulence model selection and mesh quality assurance can be found in literature resources (Nielsen et al., 2007). Nowadays, commercial CFD software can be used to initialize the problem, solve it according to the governing equations of the fluid dynamics and visualize the results.

There are some empirical equations to predict the airflow rate of the plume over a heat source.

For the point heat source in a bounded surrounding with temperature stratification, the equation for airflow rate of the plume is as follows (Baturin and Blunn, 1972):

$$q = 0.005 P_c^{1/3} z^{5/3} \tag{3.2}$$

While z (m) is the distance from the virtual point, and P_c (W) is the convective component of the heat load which is calculated according to the following equation:

$$P_c = K P_t \tag{3.3}$$

While K is the convective heat factor and a semi-empirical value depending on the size of the heat source, P_t (W), is the total power of the heat source, including the radiation term. When the supplied airflow rate is known, it is possible to find the location of the stratification height. Mundt (1996) has explained different methods of determining the flow rate of plumes over heat sources.

The heat is mainly transferred in a room by two methods, convection and radiation. In order to avoid the complication of simulation by radiation, a method is used that consider just the convective term of the heat source as a total power of the heat source. Subsequently, it is necessary to rectify the wall temperatures and use those temperatures as boundary conditions of the walls in the simulation. The surface temperatures are obtained from the experiments. The method is illustrated in Figure 3.3.

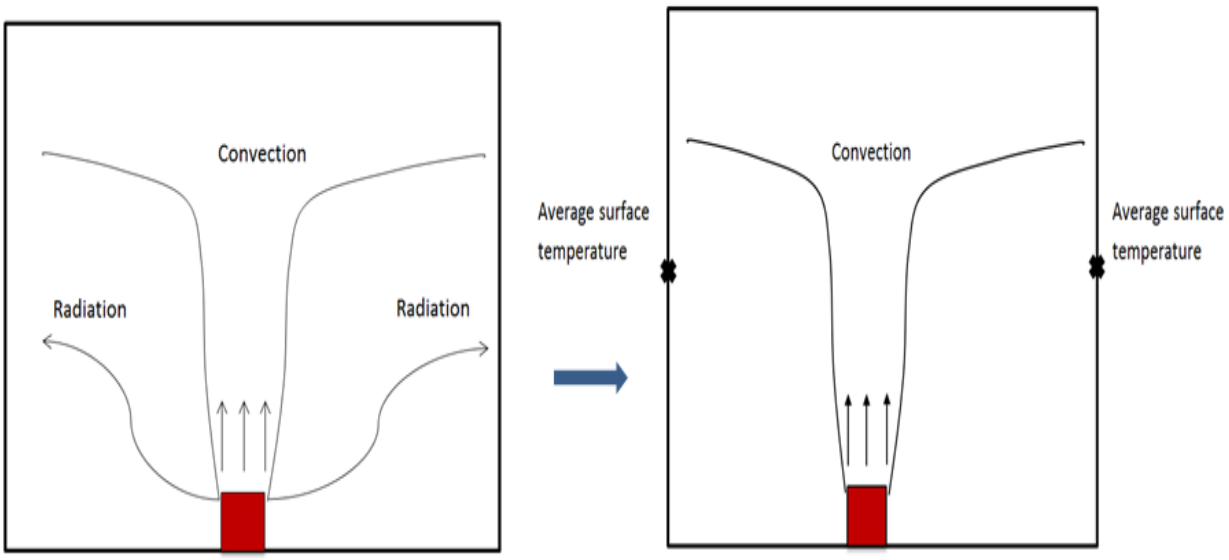

Figure3.3 Illustration of substitution of the radiation effect of average surface temperatures obtained from the experiment

Pollutants including gasses and particles exist in indoor environments. They can be generated inside the room, or they can be delivered to the indoor space by the supplied air. When the pollutant source is very close to the heat source, or when it is combined with the heat source, it is called a thermal pollutant source. Alternatively, if the pollutant source is away from the heat source, it is called a passive pollutant source. Pollutant distribution in a displacement air distribution system has been investigated by researchers. It has been established that in the case of the thermal particle source, the zone above the stratification height, i.e. the recirculating zone, has a higher particle concentration than the zone below the stratification height. However, the particle dispersion in the room with a passive particle source has been investigated in few cases and mainly experimentally.

3.2. An overview of computational fluid dynamics

As regards fluids, there are mainly three methods to solve the problems: experimental, theoretical and computational. Theoretically, there are partial differential equations to find velocity components, pressure and temperature. However, since in the best case, the number of unknowns is equal to the number of equations, no exact solution can be achieved. Instead, there is a possibility to use computational method to handle the fluid dynamics problems.

The CFD method can determine numerical expression of the flow properties of interest. In this method, the flow domain is divided into small cells which are called meshes, and the action of dividing the domain into meshes is called meshing.

It is clear that simulation of a multiphase flow is still far from reality if one wants to model all interactions between the dispersed phase and the continuous phase. For example, a non-spherical particle has a rotational behavior; it exchanges electrical charge with the surroundings and exchanges water content by condensation and evaporation. In all existing approaches, there are a lot of assumptions and simplifications (Crowe, 2005). In the following section, the simulation of particle phase, existing models and limitations in the simulation of particle phase will be discussed.

3.3. Simulation of particle phase

Bubbles, droplets and solid particles are considered as particle phase in CFD simulations. The behavior of a particle is studied according to its interactions with the surroundings. Every single particle has its own shape, chemical composition, volume and weight (Friedlander, 2000). Therefore, in order to simulate the real behavior of dispersed particles in a continuous flow, it is essential to have a grid which is so fine that the forces acting on each single particle can be calculated. This method of simulation of particles is called the Resolved-Surface method. In an ordinary office room, thousands of particles exist in a cubic centimeter of air. Consequently, simulating this large number of particles with such fine grids is practically impossible. Figure 3.4 shows the behavior of the air molecules around spherical particles. If a CFD simulation aims to simulate these three particles exactly as it happens, the mesh size should be fine enough to predict the forces exerted to the sides of the particles.

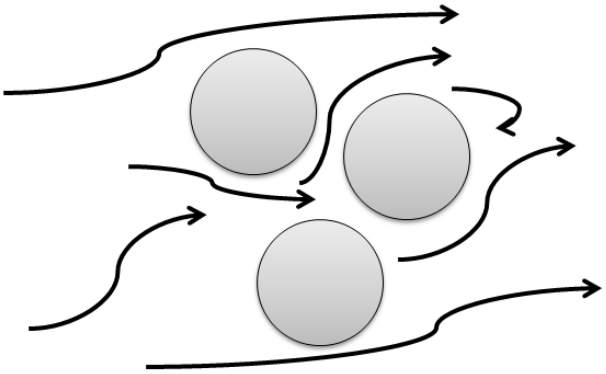

Figure 3.4 Behavior of air molecules around particles

In addition, there is still a lack of knowledge regarding the behavior of particles in the air. Some phenomena that contribute to the dynamics of particles have been studied broadly while other phenomena have not. Resuspension of particles, coagulation and particle phase change have been evaluated in some studies, but the knowledge is not enough to know the entire reality (Boor et al., 2013). Dispersion of particle phase in a room depends mainly on the location of the particle source, air velocity at inlet, air flow rate and heating power. Knowledge regarding these phenomena is limited to some experimental studies and CFD simulations (Gao and Niu, 2007; Mundt, 1996; Nazaroff, 2004).

The movements of particles include turbulent diffusion and convection. However, some factors might be the main cause of particle movement depending on the sizes of particles. Diffusion is an important factor in the transport of UFPs. Because of turbulent air movements in indoor air, diffusion is the main factor only close to the walls. For larger particles, i.e. fine particles and coarse particles, inertial force and gravitational force play main roles. Depending on the size of particles,

considering particles as gas molecules in CFD simulations may cause deviation in the results to some extent (Nielsen, 1994).

The temperature stratification in a room has an effect on the profile of particle concentration in the room as well. A thermal particle source is a particle source which is combined with a heat source. Studies have shown that with a thermal particle source, the contaminant concentration in the recirculating zone is higher than in the bottom zone for a stratified room (Skistad et al., 2004).

The particle dispersion in the air is considered as a multiphase flow of a particle phase and a gas phase. The particle phase is considered as a dispersed phase in the air if the interaction of particle-fluid is the main drive for the overall transport of the particles. In case the volume fraction of particles is less than 0.001, the multiphase can be regarded as a dilute flow (Crowe et al., 2011).

In a dilute flow, if the particles do not have impact on the behaviour of fluid, this means that only the flow is the motion drive of particles. This is considered as one-way coupling. Consequently, for a one-way coupling dilute flow, the continuous phase can be solved independent of the dispersed phase. It is a great advantage regarding the computing capacity saving in the CFD simulations.

For the simulation of air in an ordinary room, the flow can be considered as dilute, since the volume fraction of particle phase is much less than 0.001. There are mainly three approaches of simulating particle behaviour, the Particle Distribution Function (PDF) approach, the Lagrangian approach and the Eulerian approach.

PDF exists in two forms. In its first form, the PDF refers to the probability density for each property of particle such as position and velocity (Buyevich, 1972a, 1972b, 1971). In its second form, the PDF includes the gas phase (carrier gas) velocity together with particle velocity (Simonin et al., 1993).

Figure 3.5 shows the velocity vectors for the particles in two approaches, Eulerian and Lagrangian. As is shown in the figure, the Lagrangian approach includes trajectory calculations of the particles mainly for a large number of them moving through the continuous phase, while in the Eulerian approach, particles are considered as a continuum-like phase.

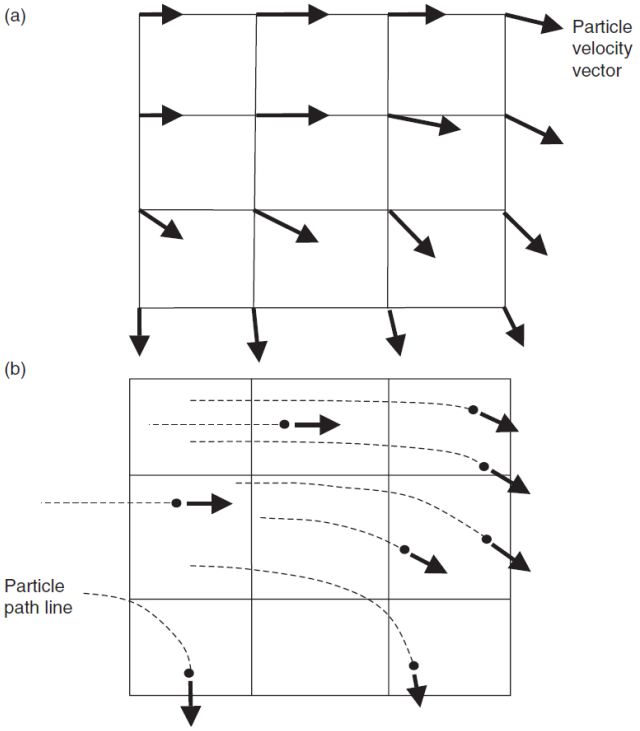

Figure 3.5 Illustration of velocity vectors in two multiphase approaches a) Eulerian b) Lagrangian (Crowe, 2005)

In the Lagrangian approach, the continuous phase is solved by an Eulerian method, and the dispersed phase is solved by a Lagrangian method. The motion of a large number of particles (particle cloud) is simulated together as a parcel in the Lagrangian approach in order to have a statically meaningful result. Tracking trajectories of a large number of particles is time consuming and expensive as regards the computing capacity.

3.3.1. Lagrangian approach

In the Lagrangian approach, the properties of a particle are calculated using simple equations of classical mechanics. The equations of motions for the particle phase are expressed as below.

$$\ddot{x} = \frac{f_b + f_s}{m} + g \tag{3.4}$$

Where $\ddot{x}$ (ms^{-2}) is the acceleration of the particle, x (m) is the position of the particle, f_s (N) is the representative of surface forces, f_b (N) is fluid force exerted on the particle, i.e. body forces, m (kg) is the mass of the particle, and g is the gravity acceleration vector. f_b (N) includes drag forces, pressure gradient force and virtual mass force.

The forces exerted on the particles include drag force, gravitational force, pressure gradient force and virtual mass force. In the indoor air conditions, the effects of the pressure gradient force and

virtual mass force are negligible as they depend on the ratio of the density of the air to the density of the particle which is about10^{-3} (Zhao et al., 2004).

Angular motion of a particle is calculated using the following equation.

$$\dot{\omega} = \frac{M}{I} \tag{3.5}$$

Here, the particle angular acceleration is shown by $\dot{\omega}$ (rads^{-2}), torque exerted on the particle by M (Nm) and inertia moment of the particle by I (kgm^2). The angular velocity and the acceleration of the particle can be counted from equations 3.4 and 3.5. Knowing the initial velocity and the time step, it is possible to calculate the particle velocity and position.

The particles are simulated in the number of steps, of which the equation of motion is as below (Maxey, 1983).

$$m_p \frac{dv_j}{dt_p} = m_p \frac{(u_j - v_j)}{\tau_p} + (m_p - m_f) g_j \tag{3.6}$$

Where j=1,2,3 showing the coordinates in three dimensions respectively, and v is particle velocity, u (m/s) is fluid velocity at particle location, m_p (kg) is particle mass and m_f (kg) is the mass of flow displaced because of particle volume. Time step of interest is shown by τ_p (s).

3.3.2. Eulerian approach

In the Eulerian approach, the particle is considered as a continuous medium with similar properties. Therefore, the equations which are used for the particle phase are similar to those of the fluid phase. Consequently, the approach is cost effective, and the procedure to find the particle properties is analogous to those of fluid. However, there are some problematic issues such as boundary conditions and poly-disperse simulation for particles, which the Eulerian method cannot handle very well (Loth, 2000; Guha, 2008). In the Eulerian approach, the properties are calculated for a computational volume of the flow (Crowe, 2005).

Both of the particle phase approaches have been used for the simulation of the particles of indoor air.Various studies have been conducted on these models, combined with different turbulence models for different particle sizes (Vegendla et al., 2011; Zhang and Chen, 2007). In most studies, the simulated particle sizes are in the range of fine particles or coarse particles, i.e. particles larger than 100 nm but not the size of UFPs.

3.4. Methodologies

In this study, a real room was selected to be simulated by commercial CFD software, *STAR-CCM+*, which is produced by the *CD-Adapco* Company. The real room dimensions were 5m×2m×2.9m. Figure 3.6 shows a three-dimensional schematic figure of the room. The red line in the figure indicated the inlet, which is a slot inlet with the dimensions of 4cm×53cm and an aspect ratio of 13.

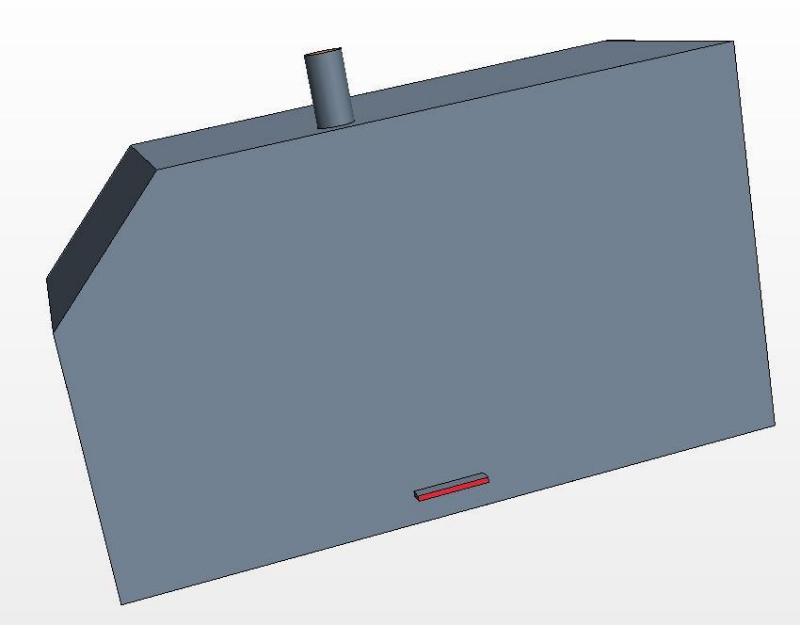

Figure 3.6 Three dimensional schematic picture of the simulated room

In order to compare the removal rate of particles and the air change rate in a room, an investigation was performed in the room. The tracer gas, N_2O, was released inside the room, and the decay of the tracer gas was measured to be 1.6 h^{-1}. Particles were generated by a candle in the room, and the decay rate of particles was measured by SMPS. As shown in Figure 3.7, particles with a diameter of less than 73 nm had a higher decay rate than the decay rate of the tracer gas, while particles larger than this size had a lower decay rate than the decay rate of tracer gas. Moreover, the fine particles had a similar decay rate compared with the tracer gas decay rate. Therefore, assuming particle behaviour identical to the behaviour of tracer gas does not result in large inaccuracy. Particles smaller than 73 nm have a higher decay rate than the tracer gas decay rate.

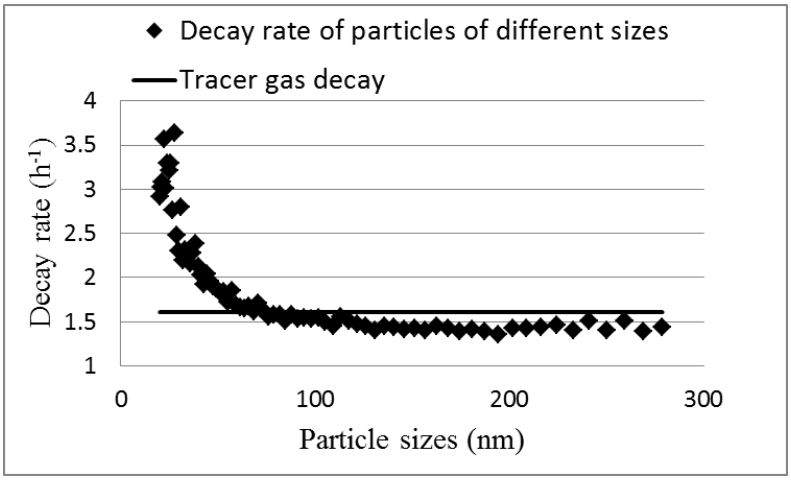

Figure 3.7 Decay rate of particles compared with the decay rate of tracer gas

The weighted mean for the decay rate of all particles was determined by averaging the decay rate of the particles of different sizes by considering the number of each size. The weighted mean decay rate for the particles was 1.63 (h^{-1}), which was very close to the number found for the tracer gas decay rate, i.e. 1.61 (h^{-1}).

The inlet velocity of the room was set to 0.3 m/s. The air movement from the inlet of the room was measured and visualized by smoke in the room to be used later for the assessment of turbulence model results.

3.4.1. Air cleaner location in a room

In the first study, the Lagrangian multiphase model was selected to evaluate the impact of the location of an air cleaner on the particle concentration inside the room. A log-normal distribution was considered for the particles with the source location close to the floor. The particle-size distribution was determined according to the size distribution that was found using the SMPS particle counter.

For the air cleaner, three different locations were simulated with the *k-ε* model, while the particle movements were simulated by the Lagrangian model. A schematic view of the layout of the room and the three locations of the air cleaner are shown in Figure 3.8. The first place was the place furthest away from the inlet and outlet. The second location was close to both the inlet and to the outlet. The third location was at the other side of the room and far from both inlet and outlet.

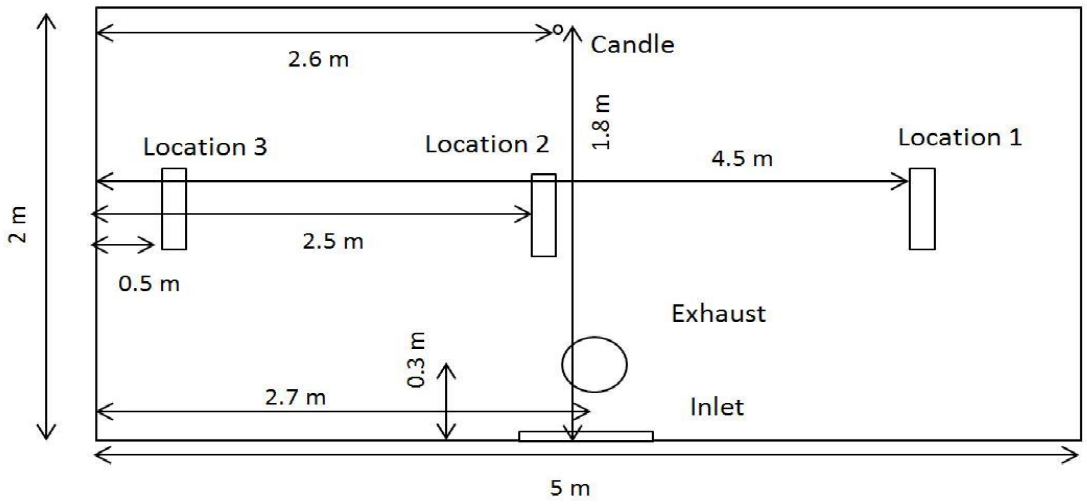

Figure 3.8 Plan view of the room, including locations of the air cleaner and the candle (Paper V)

3.4.2. Location of particle source and heat source

The second part of the study was performed to evaluate the effect of location of a heater on the distribution of UFPs in a room. Additionally, the effect of the location of a particle source was studied.

The heater was placed at the heights 0.1 m or 0.5 m. In order to evaluate the predicted temperature profile by CFD, temperature loggers were mounted at specific heights in the room. The logged

temperature data was compared with the CFD simulation. The locations of the heat source, particle source and the sampling points are illustrated in Figure 3.9.

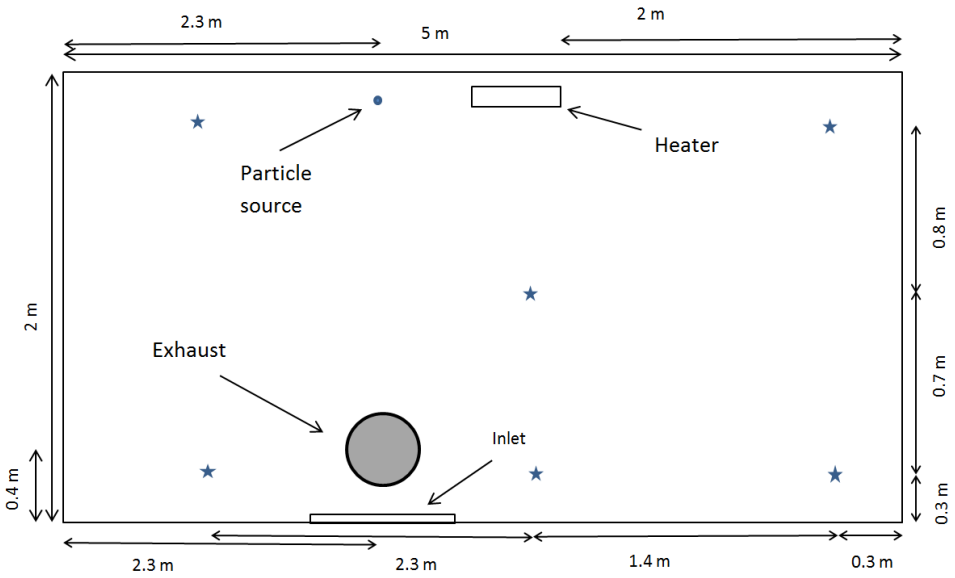

Figure 3.9 Outline of the room including heater location, particle source and sampling points (stars) in the CFD simulation (Paper VI)

In the CFD, the meshes were generated by tetrahedral meshing for room geometry similar to the real room. The number of meshes at the beginning was 400,000. The quality of mesh was improved sufficiently to achieve a grid-independent solution for temperature and velocity magnitude (Roache, 1994).

The process the grid-independent solution was repeated for the particles as well. The mesh grid was refined until reaching the solution at which it was independent of the grid size. Using the Lagrangian method, it was necessary to refine the mesh further. The number of meshes was increased to 3.2 million meshes. Similarly, in order to determine the number of sub-steps to follow the particle trajectory in the domain, the number of sub-steps was increased until reaching the independent solution. The number of sub-steps was 1.5 million.

Subsequently, the simulation was run with the turbulence models, k-ε and k-ω. After comparing the results of both models with measurements and smoke visualizations, the k-ε model was selected. In order to study the effect of the radiation on the flow pattern and the particle distribution in the room, two cases were considered regarding the radiation effect, one without radiation solver and one with radiation solver.

The process of selecting the generation rate of the particles was the same as it was increased until the particle concentration profile in an arbitrary place remained unchanged after increasing the generation rate. The particle source was located at three heights. The rate of particle generation was 20 parcels of particles in the room with the total generation rate of 50,000 particles per second. As the particles are UFPs dispersed in the air, the particle-particle interaction was not considered in the simulations.

3.5. Results

The CFD simulations were performed by the two turbulence models *k-ε* and *k-ω*. The predictions of the velocity profile close to the air inlet were compared with the experiment results. Figure 3.10 shows the results of the prediction by the two turbulence models and the experiment result.

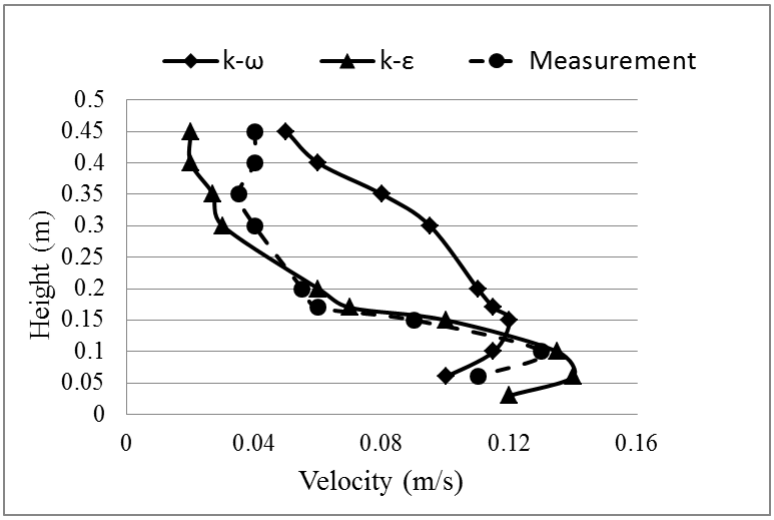

Figure 3.10 Prediction of velocity profile at a distance of 1 m in front of the inlet by *k-ε* and *k-ω* compared with the measurement results (Paper VI)

The aim of this CFD study was to investigate the possibilities of improving indoor air quality regarding removal of ultrafine particles by air cleaners. The aim was also to know the impact of the location of a heat source and a passive particle source on the distribution of ultrafine particles at different heights. Therefore, two phases of simulations were implemented. The first phase was to examine the effect of the location of an air cleaner on its particle removal effectiveness in a room. The second phase was to examine the impact of the height of a heat source and the impact of the height of a particle source on the UFP distribution in a room.

For the first phase, the average concentration of the particles in the room with ventilation but without air cleaner was designated as C_0 (UFP/cm^3). The average concentration of the particles in the room for the other three cases was designated C_1, C_2 and C_3 respectively.

The improvement of the removal effectiveness for Locations 1, 2 and 3 is calculated using Equation 3.7.

$$I = \frac{C_0 - C_i}{C_0}\% \qquad i = 1,2,3 \tag{3.7}$$

Here, *I* (%) is the increase of particle removal effectiveness of the ventilation system together with air cleaner, compared with the ventilation of the room alone. The result is shown in Table 3.1. It is seen that air cleaner in Location 2 caused the highest increase in effectiveness as compared with the two other locations.

Table 3.1 Effectiveness of different locations for the air cleaner (Paper V)

Parameter	Location 1	Location 2	Location 3
Distance to particle source (m)	2.6	1.4	2.65
Improvement by the air cleaners (%)	26	27	23

In the second part of the simulations, the effect of the height of a heat source and the impact of the height of a particle source were studied.

To compare temperature profiles of different cases, a non-dimensional temperature has been used with the following equation:

$$\theta = \frac{(T - T_S)}{(T_E - T_S)} \tag{3.8}$$

Here, T (°C) is the temperature of an arbitrary place, T_S (°C) is the temperature of supplied air to the room and T_E (°C) is the temperature of air in exhaust.

The temperature was measured in the room and then compared with the CFD results for both cases of the heater at heights 0.1 m and 0.5 m. By introducing dimensionless temperature, it is possible to draw a schematic illustration regarding temperature gradient and compare different cases. In order to validate the CFD simulation, a temperature profile along a vertical line was obtained in the real room, and this was compared to the predictions of the two turbulence models *k-ε* and *k-ω*. The results are shown in Figure 3.11. The results are for the two cases, heater at heights 0.1 m and 0.5 m. The *Radiation* model was added to *k-ε* model, and the result is compared with two basic models *k-ε* and *k-ω*.

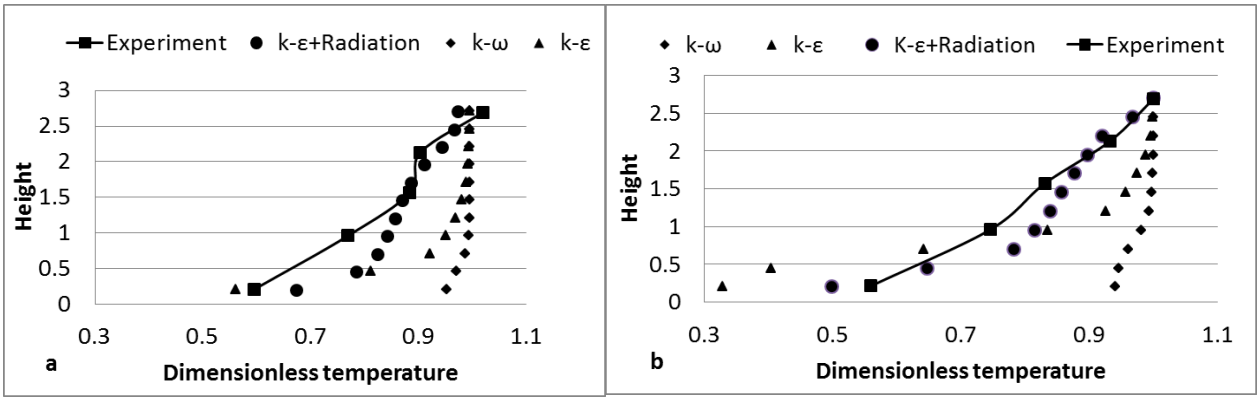

Figure 3.11 Measured and predicted temperature profile of a vertical line in the room a) heater is at height 0.1 m, b) heater is at height 0.5 m (Paper VI)

The stratification heights of the two cases were calculated according to equation 3.2. The predicted stratification height by CFD simulation and the calculated stratification height are shown in Table 3.2.

Table 3.2 Calculated and predicted stratification heights (Paper VI)

	Stratification height (m)	
Method	Heater at 0.1m	Heater at 0.5m
Calculated by equation	0.4	0.8
Prediction by *k-ε*	0.35	0.7
Prediction by *k-ε+ Radiation*	0.45	0.75

For the two locations of the heater, the CFD predictions by both turbulence models *k-ε* and *k-ω* were compared with the experimental result for an arbitrary vertical line far from the heat source and the particle source. Subsequently, the average value of particle concentration in the room for two heights of particle sources was calculated according to the CFD predictions. The particle source heights are 0.2 m and 1.5 m.

The CFD prediction of particle concentrations for the vertical line when the heater is at the height of 0.1 m is shown in Figure 3.11.

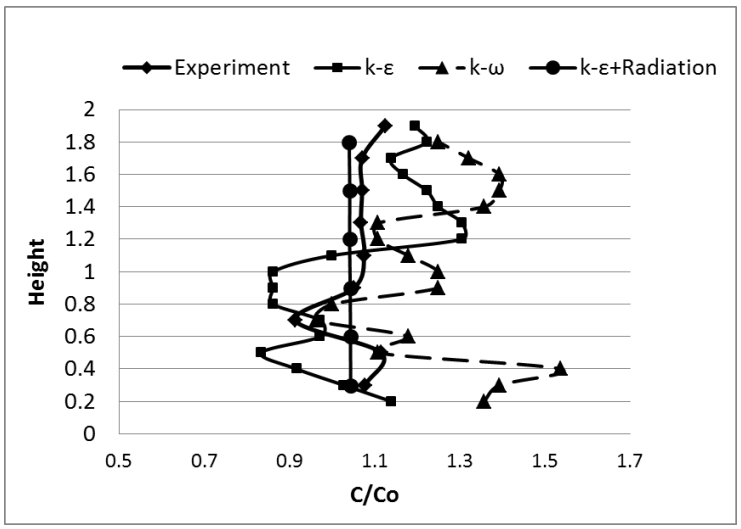

Figure 3.12 Predicted average particle concentration profile and measured in the room when the heater is at height 0.1 m and the particle source is at 0.2 m

According to the results shown in Figure 3.10, Figure 3.11 and Figure 3.12, the *k-ε* model predictions better matched to the experiment results. Therefore, this model was selected as turbulence model for further simulations of the case with the heater at the height of 0.1 m.

The focus of this study was on the average particle concentration in the room. For several heights in the room, the average particle concentration was obtained. For each height, the average particle concentration was calculated by averaging the particle concentrations of the points shown in Figure 3.9. The average predicted concentrations of particles while the heater is at the height of 0.1 m and the particle source is at 0.2 m and 1.5 m are shown in Figure 3.13 from left to right respectively. The vertical lines that were selected close to the wall near the particle source and heat source showed higher particle concentrations than the other vertical lines.

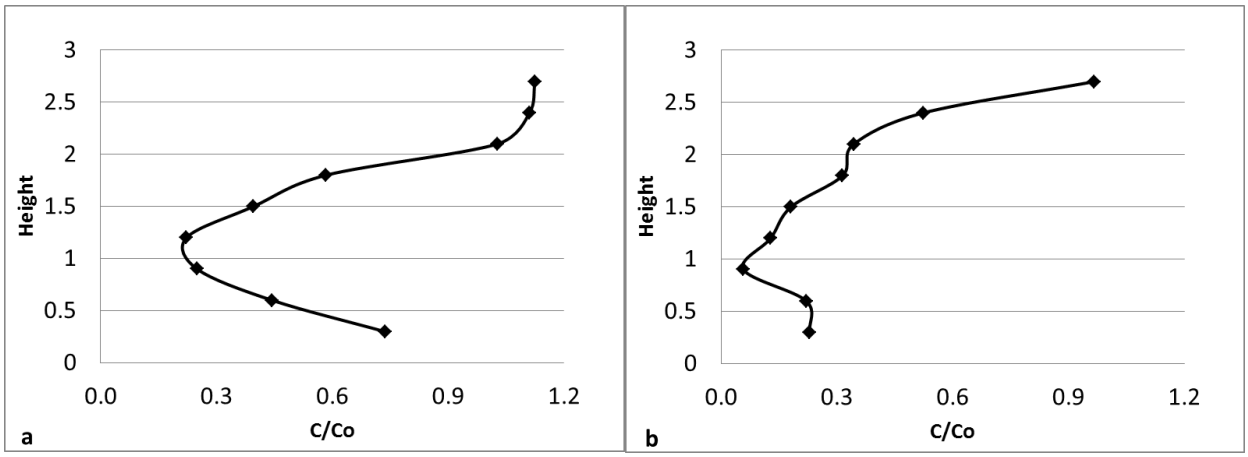

Figure 3.13 Predicted average particle concentration profile by *k-ε +Radiation* when the heater is at height 0.1 m and the particle source at heights a) 0.2 m b) 1.5 m

The heater was moved to the height of 0.5 m and the same procedure was carried out regarding mesh refining and solution. The predicted concentration of particles for an arbitrary vertical line was compared with the experiment results. Figure 3.14 displays the CFD prediction by both turbulence models *k-ε* and *k-ω* and the experiment results.

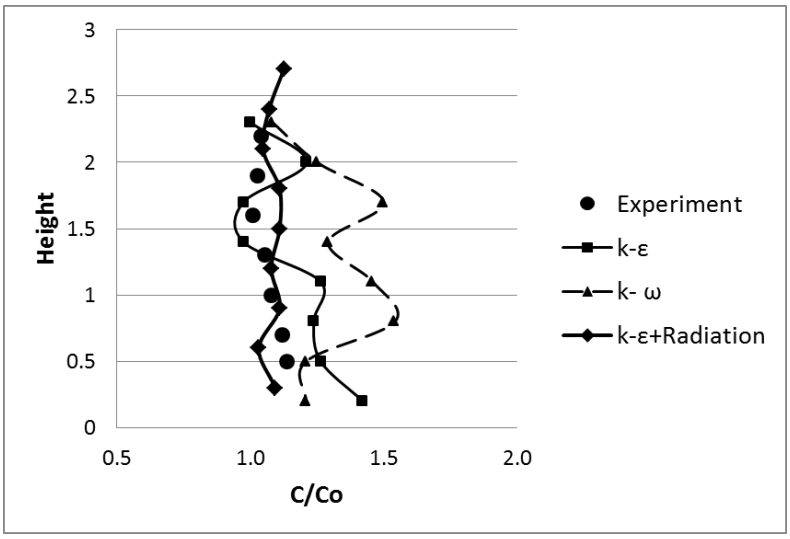

Figure 3.14 Predicted average particle concentration profile and measured particle concentration in the experiment in the room when the heater was at height 0.5 m and the particle source was at 0.2 m

According to the results shown in Figure 3.14, it seems that with the Radiation model, *k-ε* shows similar results to that logged in the experiments for the case in which the heater is at the height of 0.5 m.The average predicted concentrations of particles for the vertical line while the heater is at the height of 0.5 m and the particle source is at 0.2 m and 1.5 m are shown in Figure 3.15 from left to right respectively. According to the results the points close to the particle source show a higher concentration profile than the remote points. But here just the average of all points is reported.

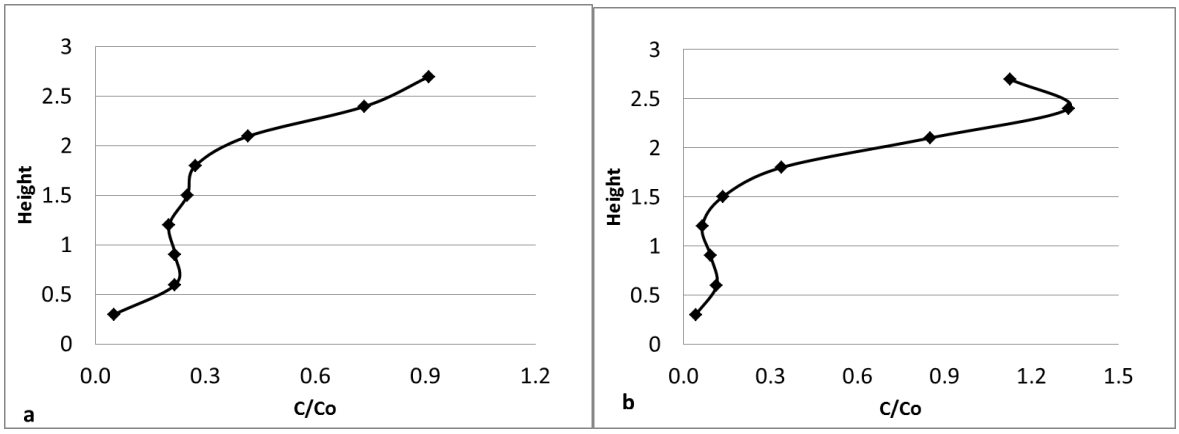

Figure 3.15 Predicted average particle concentration profile by *k-ε +Radiation* when the heater is at height 0.5 m and the particle source at heights a) 0.2 m b) 1.5 m

4. Discussions

The results which presented in the previous chapters of the experimental investigations and simulation of particle dispersion in a room are discussed in the present chapter.

4.1. Experimental investigations on air cleaning technologies

The investigation on the air cleaning technologies shows that the three air cleaning technologies CDI, NTP and PAP increased the ozone concentration in the clean room. According to the results, the level of ozone was increased by 44%, 33% and 11% with NTP, CDI and PAP respectively. It is clear that the ozone concentration generated by PAP was lower than for the two other technologies i.e. NTP and CDI (Paper I).

As explained in section 2.2.2, the air cleaners NTP and CDI use a high voltage discharge method to inject the electrons into the air. By exciting the passing air including oxygen molecules, the air components start reactions including the generation of ozone.

The maximum ozone concentration caused by an air cleaner has been evaluated, and some equations have been proposed (Niu et al., 2001; Tung and Niu, 2005). Using a mass balance equation, it is possible to estimate the maximum ozone concentration caused by an air cleaner, if ozone generation rate and ozone removal rate by surfaces and ventilation system are known. The generated ozone molecules are unstable and react with other components including VOCs.

One finding in the present study was that NTP and PAP air cleaning technologies increase the concentration of UFPs after the ozone concentration has been increased by the cleaners in the clean room. According to the data of particle concentration in the room, CDI did not increase the level of

UFPs inside the room. PAP increased the ozone less than two other technologies, while it increased UFP concentration significantly.

One possible mechanism of increasing and later decreasing the level of UFPs may have been the secondary formation of particles, since unsaturated VOCs might react with generated ozone (Alshawa et al., 2007; Hubbard et al., 2005; Waring et al., 2008). The VOCs are added to indoor air by different sources such as building materials, cleaning products and outdoor sources (Edwards et al., 2001; Knudsen et al., 1999).

The UPF concentration in the room increased up to a maximum concentration and then it started to decline. There seems to be specific substances in the air that reacted with the ozone. The concentration of UFPs decreased slowly by decreasing the concentration of these substances in the room. In addition, the level of UFPs continued to be at a steady-state. A steady-state particle concentration higher than the background concentration seems to be achieved since the VOCs are entered to the clean room through the supplied air. So, the reactions between ozone molecules continued. However, the number of reactions was reduced because of the reduction in the number of unsaturated VOCs in the air. Therefore, it seems that the first possible mechanism is likely to be true.

The experiment was repeated in winter for the PAP technology. The maximum level of generated UFPs in winter was 5000 (UFP/cm^3). This was lower than the maximum particle concentration in the summer measurement. One of the sources of VOCs such as terpenes is trees. The trees emit less VOC in the winter time than in the summer time. Therefore the reason seems to be a lower level of unsaturated VOCs in the air in winter compared with summer. According to the logged data for TVOC in winter, its level is lower than the level of TVOC in summer.

In addition, there was no significant increase in the concentration of UFPs for the CDI technology. The reason seems to be that CDI itself can eradicate the generated particles, and therefore the concentration of UFPs was not increased.

The results of the evaluation of ozone and particle generation by the air cleaners can be considered as a basis for studying and modelling the ozone and particle generation of the air cleaners in an ordinary room with furniture and other material (PaperI).

The effectiveness of the air cleaning technologies was also evaluated in the clean room and in the office room. Table 2.3 shows the effectiveness of the air cleaning technologies in removing UFPs when the air cleaners were placed in the clean room. By performing two experiments for each air cleaner, one without air cleaner and one with air cleaner, and subtracting the two removal rates, the effect of deposition is eliminated. Table 2.4 shows the results of the experiments performed to determine the effectiveness of the air cleaning technologies placed in an office room. According to the table, the effectiveness of the EFF is the highest. However the two other technologies 3D Filter and CDI have the effectiveness very close to that of EFF.

According to the experiments of both clean room and office room, EFF has the highest effectiveness. In contrast to of NTP, CDI and PAP, this technology does not generate ozone. According to the experiments, it does not increase the level of UFPs eigther. The measured pressure drop of EFF is less than 5 Pa.

Further experiments with EFF technology were carried out, focusing on its efficiency in removing UFPs. According to Figure 2.10, the EFF filter has a higher efficiency in the capture of smaller UFPs as compared with larger UFPs. This is due to the fact that when increasing the size of the particles, the effect of diffusion in the capturing of the particles by the fibers of the filter decreases.

According to the experiments using candle particles, filter efficiency increases by increasing the UFP exposure. Some hypotheses have been made to explain this phenomenon of varying the efficiency. One hypothesis is that it is because of an error caused by the particle counting instruments. NanoTracer counts the particles according to the charge taken by the particles. SMPS has a CPC which uses light scattering to count the particles. This hypothesis seems unlikely to be true, since the counters use different methods to count the particles and they show the same trend.

Another hypothesis is that when increasing the concentration of the particles, the number of particle dendrites on the fibers increase, and consequently they contribute in the process of capturing the other particles. After impingement of the first particle to the filter fiber, there is a high probability that the particles attach on this particle and construct some chain like shapes called as dendrites. Tien et al. (1977) introduced a theory to explain the way of forming a dendrite on a fiber located in a flow stream. As shown in Figure 4.1, after the first particle (a) has settled, following particles (b_1 and b_2) will attach to the first particle, if their trajectory targets a point in the arc of B_1B_2 shown in the figure. This phenomenon is called the shadowing effect.

As regards the interception and impaction effects, it has been possible for researchers to propose some theoretical explanations to predict the dendrite shape and the rate of its formation (Payatakes and Tien, 1976; Payatakes, 1977).

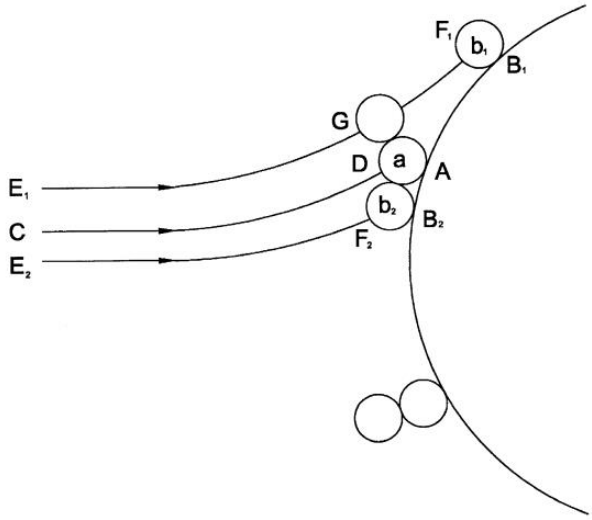

Figure 4.1 Shadowing effect and chain-like deposition (Wang, 2001)

In order to examine the validity of the hypothesis, in the second step of experiments, measurements were carried out on the filter. According to the inspections via microscopic investigations, the numbers of constructed dendrites on the fibers change by the concentration.

In order to scrutinize whether the electrostatic charge of the fiber surface plays an important role in the efficiency change, the test was implemented using salt particles. The salt particles are made of inorganic material and are water soluble, and they are considered to be good electrical conductors. Therefore, they prevent the accumulation of a surface static electrical charge. According to Table 2.5, with salt particles, there is no correlation between the particle concentration and the filter efficiency. Probably, the number of dendrites is low for salt particles.

In addition, the filter efficiency for salt particles is lower than the filter efficiency for candle particles. This difference is due to the difference between candle particles and salt particles regarding electrostatic charge. The candle particles are charged more effectively than the salt particles as wax is not a good conductor. This facilitates the build-up of a good surface electrical charge on the candle particles and improves the capturing efficiency of filter fibers. Therefore, it is concluded that particle composition, in addition to size, is an important factor in changing filter efficiency. Static electrical charging of dendrites will spread out the branches, increasing the capture of the rest of the particles.

Figure 4.2 shows photos of the filter fibers exposed to the different particle concentrations. Figure 4.2a shows a fiber of the filter piece that was subjected to particle exposure lower than 3.0E+4 UFP.mincm^{-3}, i.e. a low level. The surface of the fiber was clean with a low number of captured particles. Some large particles could also be detected as shown in Figure 4.2a. Figure 4.2b shows a fiber which was exposed to 1.2E+5 UFPmincm^{-3}, i.e. a medium level. The surface of the fiber was clean; however, it was possible to see the nucleation of particle dendrites on the fiber. Figure 4.2c shows a fiber which was loaded by 1.5E+6 UFPmincm^{-3}, i.e. high level of particle exposure. Few dendrites could be seen on the surface of the fiber. As shown in the figure, some of the dendrites rested parallel to the fiber. Figure 4.2d shows a filter that was loaded to 3E+6 UFPmincm^{-3}, i.e. a high level. As shown in the figure, many dendrites formed on the surface of the fiber.

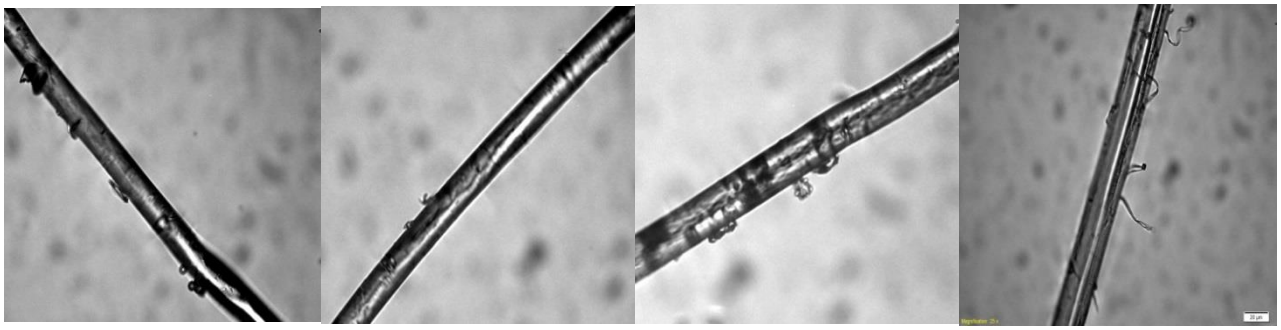

Figure 4.2 Photos from the filters with varying exposures a) <3.0E+4 b) 1.2E+5 c) 1.5E+6 d) 3.0E+6

Bearing in mind the existing theories explaining particle deposition on a filter media and considering the current investigation, it seems that more investigations are needed to elucidate the phenomena contributing in the capturing of UFPs by an electrostatically charged filter.

The EFF filter was combined with a chilled beam and then was tested to see whether this would increase the rate of the UFP removal inside a room (Paper IV). As shown in Figure 2.13, the UFPs were removed faster in the combined system compared with the chilled beam. The removal rate of the UFPs increased 2 h^{-1}.

For both cases, the tracer gas technique was used in order to study how much the airflow rate in the room was reduced. The pressure loss through the filter was measured, and it ranged between 2.5 and 3.75 Pa. It was possible to estimate the total air change rate caused by the filter. The total air change rate for a combined system can be calculated using the following equation:

$$ACH_{combined} = ACH_v + ACH_f \quad (4.1)$$

Where $ACH_{combined}$ (h^{-1}) is the particle removal rate of the combined system, ACH_v (h^{-1}) is the particle removal rate of the ventilation system including deposition and ACH_f (h^{-1}) is the particle removal rate by the filter. The particle removal rate was calculated by the following equation:

$$ACH_f = \frac{(E_f \times Q_f)}{V} \quad (4.2)$$

Where E_f is particle removal efficiency, Q_f (m^3/h) is air flow rate passing through the filter, i.e. induced secondary airflow, and V is the volume of the room.

The magnitude of Q_f was calculated as 126 l/s by measuring the velocity of the secondary induced airflow and multiplying by the cross-sectional area of the chilled beam. Assuming the efficiency of the filter to be 78%, ACH_f was calculated to be 1.93 h^{-1} according to Equation 4.3.

Therefore, the particle removal rate predicted for the combined system is 4.63 h^{-1}, which is similar to the outcome of the experiments, i.e. 4.7 h^{-1}. Knowing the efficiency of the filter and the secondary airflow rate of the chilled beam, it is possible to calculate the total particle removal rate of the filter, and the total air change rate for the combined system.

Reduction of the airflow rate had the reverse effect on the performance of the chilled beam as a device to exchange the heat. However, this must be evaluated considering the increase in the CADR of the filter for particles. As shown in Table 2.6, using the filter to remove UFPs from the secondary induced airflow caused a reduction of the sensible heat removal effect of the chilled beam. The reduction of the effect ranged between 22% and 38%. The reason was that due to the pressure loss caused by the filter, the amount of the induced airflow decreased.

4.2. Simulation of particle dispersion in a room

4.2.1. Air cleaner location in a room

One of the methods of treating pollution in indoor air is cleaning the air. Portable air cleaners can be used in a room to remove pollutants. The concern arising is that what the impact of the placement of an air cleaner is on its effectiveness. According to the result expressed in Table 3.1, the location of an air cleaner has only a small impact on the average particle concentration. Changing the location of an air cleaner will change the air distribution in the room and consequently the average particle concentration in the room. However, the change is not significant according to the results.

The effectiveness of an air cleaner has been studied by researchers and some equations have been introduced. One equation has been introduced by Nazaroff (2000). In this equation, it is assumed that the air is fully mixed and the location of an air cleaner is not considered as an important factor. According to the result shown in Table 3.1, the assumption in the equation seems to be reasonable.

4.2.2. Location of particle source and heat source

The other method of treating pollution in indoor air is diluting it by a ventilation system. It is very important to understand the impact of the heat source height and the particle source height on the dispersion of UFPs in an indoor environment.

Figure 4.3 shows the vertical temperature profile in the room simulated with three inlet velocities, 0.2 m/s, 0.4 m/s and 0.7 m/s. As shown in the figure, by increasing the inlet velocity from 0.2 m/s to 0.4 m/s, the stratification height is raised. By changing the velocity to 0.7 m/s the temperatures at all heights remain almost the same. This shows that by increasing the inlet velocity to above a

specific level, the air becomes fully mixed in the room and the temperature profile becomes similar to the mixing air flow pattern. This is a sample to show how hard the prediction of an air flow pattern in a room is.

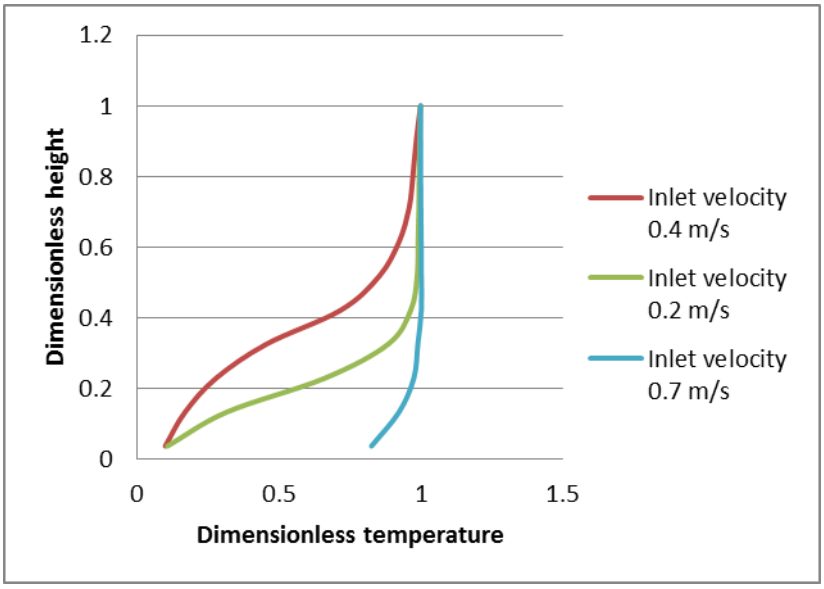

Figure 4.3 Effect of the inlet velocity on the vertical temperature profile in the room

Without considering radiation effect, the predicted UFP concentration profile for a vertical line in the simulated room differs than that is expected for the case that the particle source is thermal particle source. The CFD with radiation predicts a higher concentration at the heights about 1 m, while the measurement does not show any significant difference.

Figure 3.11 shows predicted and measured temperature profiles in the room. It is clear that the CFD simulation without considering the radiation effect predicts a higher temperature at the same height compared with the measured temperature. Without considering the radiation effect, the mixing in the room is predicted to be less than that which is obtained according to the experiments.

While, by considering the radiation effect, prediction is similar to the experiment result. Radiation causes local turbulences close to the walls and therefore increases the total mixing in the room. The experiment result shows higher mixing in the room. This seems to be because the temperature loggers were also affected by the radiation heat transfer from the heater and candle, and therefore they might also record a higher temperature and cause the experimental data to deviate from CFD results.

Furthermore, without considering the radiation effect, the measured ultrafine particle concentration profile and the simulated profile differed more than expected for turbulence models, k-ε and k-ω.

The simulations made by the k-ε model show results closer to experimental results compared with the k-ω model. As shown in Figure 3.11, by changing the height of the heat source, the predicted temperature profile by k-ω does not show any change.

After adding the radiation effect to the k-ε model, the result is similar to the experiment result. There is a method of simulation that neglects the radiation effect of a heat source and for compensation of radiation effect sets the temperature of the walls equals to that determined by the

experiment. As shown in both Figure 3.12 and Figure 3.14, the *k-ε with Radiation* model predicts a concentration profile similar to the experiment result. Therefore, neglecting the radiation effect and just considering the convection of a heat source causes discrepancy in the predictions of the particle concentrations.

According to Table 3.2, the predicted stratification height by CFD simulation is similar to the calculated stratification height for both cases. However, the simulation predicts higher stratification height for the case where the heater is at the height of 0.1 m and lower stratification height when the heater is at the height of 0.5.The reason could be the discrepancy caused by the assumptions in Equation 1, since it is an empirical equation with assumptions.

Figure 3.13 and Figure 3.15 show the average of the particle concentrations of the vertical lines in the shape of star signs in Figure 3. 9. Comparing the figures, it seems that by increasing the height of the heater, the average particle concentration decreases. For each vertical line close to the particle source, the concentration is higher than a vertical line far from the particle source.

The particle concentration profile for the case where the heater is at 0.1 m, and the particle source is below the stratification height, i.e. z=0.2 m, is shown in Figure 3.13 a. The particle concentration along the vertical line is high in the zone below the stratification height, i.e. lower zone. The particle concentration is also high in the zone above the neutral line, i.e. the recirculating zone, which is the area in which the plumes over the heater recirculate and cause a full mixing condition.

Comparing this figure with Figure 3.13 b, it is clear that when the candle is placed in the higher height, the lower zone has lower particle concentration. The reason is that the stratification height acts as an impermeable boundary for the particles between the upper zone and the lower zone. Therefore, it does not let the particles travel to the lower zone.

The same difference is seen between Figure 3.15 a, and Figure 3.15 b. By moving the particle source to the zone above the stratification height, the particle concentration shows a reduction in the lower zone. For the case in which the particle source is at the height of 0.2 m, the particle concentration in the lower zone decreases the height of the heat source is increased. This can be interpreted by comparing Figure 3.13 a, and Figure 3.15 a.

Since a candle is used in the experiment, the plumes generated by the candle have the mixing effect in both zones, above the stratification height and below the stratification height. The particles travel with the plumes to the upper zone. Moreover, at the height equal to the source height, the concentration is high and the profile resembles the previous measurements (Heiselberg and Sandberg, 1990; Nielsen, 1993). This is correct when the heat source and the particle source are at the same height close to the floor.

5. Conclusions and future works

5.1. Experimental investigations

It is concluded from the results of experiments on the air cleaning technologies that ozone initiating technologies may increase the ozone concentration in a room to a level higher than the maximum level allowed, which is 120 μgm^{-3} ("Air Quality Guidelines for Europe", 2000). The result showed that the particle generation rate and the maximum ozone concentration change depend mainly on the rate of air supply, the age of the building material and the size of a room.

On the basis of the results, it was concluded that the EFF filter works efficiently in removing UFPs generated by a candle or a salt source. It does not generate ozone, and it showed an effectiveness of 0.7 in removing UFPs in the clean room, while it caused a pressure drop of less than 5 Pa.

The combined chilled beam system had a UFP removal rate which was about 2 h^{-1} higher due to the existence of the filter. However, it caused a reduction of 38% in the efficiency of the chilled beam. The filter needs to be evaluated further to examine what the relation is between the filter efficiency and the filter age.

The efficiency of the EFF seems to change when the particle exposure and particle composition are changed. The efficiency of the electrostatic filter changed from 44% to 80% depending on the particle concentration and particle size. Furthermore, the efficiency of the filter in removing all sizes of particles decreases when the concentration of the particles is decreased. According to the experiment results, the main reason for the change in the efficiency of the filter when the exposure is changed seems to be the formation of particle dendrites.

In order to gain more knowledge about the correlation between filter efficiency and particle exposure and composition more investigations are required. In addition, the effect of the charge

amount of a filter on its efficiency needs to be studied. In addition, it is necessary to establish a model for the ozone initiating air cleaning technologies which also includes the condition of the room in which the air cleaner is placed. This will make it possible to predict the concentration of particles generated.

5.2. Simulations

It is concluded that the location of an air cleaner in a room location can have a small impact on the effectiveness of the air cleaner. According to the simulations, it can be concluded that when the particle source is below the height of 0.2 m or 1.5 m, the elevation of a heater height can change average particle concentration profile of a room. When the heater is placed at the height of 0.5 m the average concentration is lower than when the heater is at a 0.1 m height.

According to the results of the decay rate measurements for tracer gas and UFPs, considering particles as gas in the simulation, or considering particles of one single size will result in a deviation for particles smaller than 73 nm.

According to CFD predictions, when the particle source is apart from the main heat source, the upper zone particle concentration is higher than the lower zone concentration. However, depending on the height of particle source location and heater location, the difference can change.

More investigations are needed to complete the knowledge of the particle profile in a room and the best heater location and particle source location in order to achieve the best indoor air quality. It is also suggested that work is carried out on simulating a cooking stove case, as the cooking stove is also a particle source combined with a heat source which is broadly in use by people.

Appendix 1 Accuracy of the experiments

When depicting the result of a measurement, it is essential to report the accuracy of the experiment by a quantitative method. This provides a possibility for others who read the report to assess the result according to the quantitative accuracy report.

The uncertainty of the result of a measurement expresses the lack of exact knowledge of the value of the measured property. Apart from the concept *uncertainty*, another concept is *error* which includes systematic error and random error.

According to the definition by the International Organization for Standardization (BIPM et al., 2008), a random error "arises from unpredictable or stochastic temporal and spatial variations of influence quantities". In addition, a systematic error "cannot be eliminated but it too can often be reduced". If a systematic error arises from a known effect, it is called a systematic effect, and its impact on the results can be minimized using a correction factor.

In the current study, all the measuring devices were calibrated by legitimate organizations. In addition, the systematic effects of the measuring devices were obtained by comparing their data obtained in a single experiment with a more reliable device. The values were logged simultaneously by both devices. For those measuring devices working with different principles, the correction factors for different levels of the values were determined.

In order to determine the level of uncertainty of the logged data, two methods were used. The first method, which is called type A by the International Organization for Standardization, was based on determining the value using arithmetic mean value and standard deviation using Equations A1.1 and A1.2 respectively.

$$\bar{x} = \frac{1}{n}\sum_{i=1}^{n} x_i \quad \text{(A1.1)}$$

$$s^2 = \frac{1}{n-1}\sum_{i=1}^{n}(x_i - \bar{x})^2 \quad \text{(A1.2)}$$

In order to obtain the combined standard uncertainty, for the case of uncorrelated input quantities, following equation can be applied.

$$u_c^2(y) = \sum_{i=1}^{n}\left(\frac{\partial f}{\partial x_i}\right)^2 u^2(x_i) \quad \text{(A1.3)}$$

Here, *f* is the functional relationship between x and y.

There is another type of evaluating uncertainty which is named uncertainty type B. In this type, to estimate the uncertainty of the measured value some information is used including "previous experiment data, experience or general knowledge with the measuring device, manufacturer's specifications, data provided in calibration and other certificates" (BIPM et al., 2008).

According to the manual of SMPS, the accuracy of the concentration reading is limited by a statistical error. As the total fractional concentration decreases the statistical error increases. The error is calculated using the following equation:

$$\sigma = \frac{\sqrt{N}}{N} \quad \text{(A1.4)}$$

Where, N is the number of particles in each size fraction. Operating at high concentrations causes a CPC has an error due to the overlapping of the particles when they are scattering the light beam. The SMPS used in the experiments has built-in coincidence correction. The coincidence is multiplied to the counted number, and its magnitude changes depending on the order of counted particles.

In type B evaluation of standard uncertainty, the uncertainty of different components can be considered such as the resolution of a digital indication and finite-precision arithmetic. However, in this study, these amounts are negligible.

In the case of calculating the efficiency of a filter according to the logged concentration of particles by the particle counters NanoTracer, the uncertainty can be determined as follows. Table A1.1 shows eight UFP concentrations logged continuously by the NanoTracer, before and after a filter. By using Equation A1.1 and A1.2, it is possible to obtain the arithmetic mean and measurement uncertainty of the data.

Table A1.1 Logged data of UFP concentration, upstream and downstream of a filter

Sample number	Upstream (UFP/cm^3)	Downstream (UFP/cm^3)
S1	40722	24071
S2	41944	23121
S3	55446	22448
S4	57109	21446
S5	47640	22008
S6	49069	20086
S7	49864	20352
S8	51360	20808

The experimental uncertainty for downstream is 1389 and for upstream the value is 5777. The efficiency of a filter can be calculated by the following equation. According to the manufacturer's manual, the uncertainty of readings of NanoTracer is ±1500. This should be added to the uncertainty. Therefore, the combined uncertainty for the concentrations will be for downstream is 2045 and for upstream the value is 5969.

$$Eff = \frac{C_{upstream} - C_{downstream}}{C_{upstream}} \tag{2.1}$$

The equation can be rewritten as follows. According to Equation A1.5 the value of the efficiency depends on two variables. Therefore, in order to calculate the uncertainty of the efficiency term, combined uncertainty should be calculated.

$$1 - Eff = \frac{C_{downstream}}{C_{upstream}} = y \tag{A1.5}$$

In order to calculate the combined standard uncertainty of the efficiency, Equation A1.3 is used. However, the concentrations are upstream and downstream are correlated. By calling $C_{downstream}$, D and $C_{upstream}$, U, for a correlated y we will have the following equation.

$$u_c^2(y) = (\frac{\partial f}{\partial U})^2 u^2(U) + (\frac{\partial f}{\partial D})^2 u^2(D) + 2\left(\frac{\partial f}{\partial U}\right)\left(\frac{\partial f}{\partial D}\right) u(D)u(U)r(D,U) \tag{A1.6}$$

By calculating the partial derivatives and substituting to Equation A1.6, the following equation can be found which can be used for calculating the combined standard uncertainty.

$$u_c^2(y) = (-\frac{\bar{D}}{\bar{U}^2})^2 u^2(\bar{U}) + (\frac{1}{\bar{U}})^2 u^2(\bar{D}) + 2(-\frac{\bar{D}}{\bar{U}^2})(\frac{1}{\bar{U}}) r(\bar{D}, \bar{U}) \quad \text{(A1.7)}$$

Adding standard uncertainties and the arithmetic means which obtained from Table A1.1 to Equation A1.7, the combined uncertainty is obtained. Here, if we consider that the concentrations are independent, the correlation factor, r will be zero. The correlation factor, with arithmetic numbers can be determined by following equation.

$$r(\bar{D}, \bar{U}) = \frac{1}{n(n-1)} \sum_{i=1}^{n} (D_i - \bar{D})(U_i - \bar{U}) / (u(\bar{U}) u(\bar{D})) \quad \text{(A1.8)}$$

Here, the number of samples, n is eight. According to Equation A1.8 r is 0.07 and the combined uncertainty for efficiency is 0.46%.

In order to determine the expanded uncertainty, a coverage factor should be determined to have high coverage probability for the selected interval of the value which is estimated. For the level of confidence of 90% according to Annex G of JCGM 100 (BIPM et al., 2008), the coverage factor is considered 1.645. Therefore, the expended uncertainty of the efficiency will be 0.76%.

In the current study, manufacturer's specifications and data provided in calibration are used. In addition, the experience regarding the measuring device was also used to evaluate the data gathered.

According to the experiments, the NanoTracer showed high fluctuations in concentrations less than 1000 UFP/cm^3. This was reported in Paper II. Therefore, in all other experiments, the data of the NanoTracer for concentrations less than 1000 UFP/cm^3 was not used.

As reported in Paper II, the data of different particle counters were compared. In addition, all measuring devices were ensured to be calibrated. In order to measure the concentration of TVOC and the tracer gas, two gas monitors, Bruel&Kjær model 1302 and Innova131 were used in the experiments. An experiment was performed in order to find the correlation between the data logged by these two gas monitors.

Appendix 2 Particle simulation by Lagrangian multiphase: A benchmark

In the following text, the method of simulating particles in indoor air is briefly depicted. The models of simulating forces exerted on particles should be selected depending on the size of the particles. In the large particles shown in Figure A2.1.a, the overall force exerted by the air molecules on the particle surface (pressure difference) is important. If the particles are nano size particles as shown in Figure A2.1.b, the drag forces caused by each air molecule is important. Between these two sizes will be considered as the transient size. For the particles with this size, the models in the simulation should be selected with more caution.

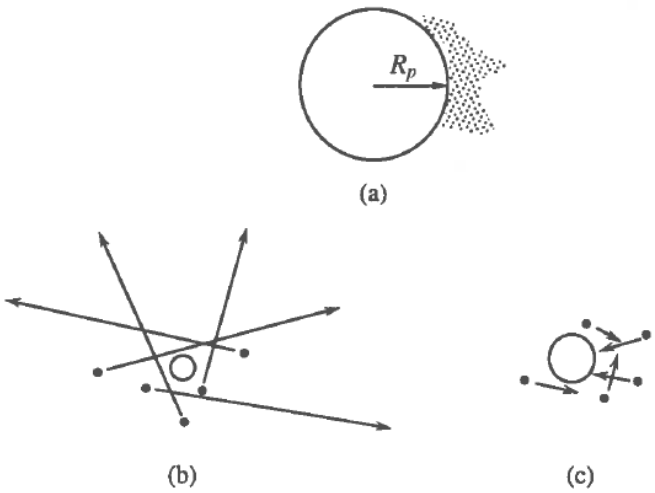

Figure A2.1 Schematic view of the interaction between particles and air molecules a) Continuum regime b) free molecule regime c) Transient regime (Seinfeld and Pandis, 1997)

Regarding the particle deposition on the walls, depending on the size of the particles to be simulated and the temperature gradient in the room, the dominant phenomenon may be Thermophoresis or Diffusion. For UFPs, the dominant force is diffusion, and for micro-size particles, the dominant force is Thermophoresis.

As the volume ratio of the particles to the air is less than 0.001, the particles can be solved as one-way coupling. This means that the effect of particles on airflow pattern is minimal. Consequently, it is possible to solve first the continuum phase and after the solution being converged, the Lagrangian multiphase will be solved.

Regardless of the methods used for solving a particle phase, it is essential to ensure that the solution is grid-independent. The process of achieving a grid-independent solution should be used for both the continuous phase and the dispersed phase. The mesh grid will be refined until reaching the solution that is independent of the grid size. Detailed information regarding the CFD application and the method of handling grid dependency can be found in the REHVA Guidebook number 10 (Nielsen et al., 2007).

When using the Lagrangian method, it is generally required to refine the mesh further for the particle simulation in indoor air. In an ordinary room the concentration of particles is in the order of 10^3. In this case, it is essential to inject a sufficient number of particles in order to ensure that the result is statistically correct.

In order to ensure that the number of particles injected and the number of parcels are sufficient, an arbitrary vertical line in the room is selected, and the profile of the particle concentration along this line is obtained for each simulation. The number of particles injected to the room will increase until the change in the particle concentration profile is negligible.

In case of the existence of a particle source combined with a heat source, the simulation of the particle source without considering the heat source will result in a prediction with a deviation. The deviation comprised two parts, deviation in the prediction of the flow pattern and deviation in the particle phase. Therefore, it is essential to consider the heating part as well. The radiation effect should be checked if it causes a dramatic prediction change.

The predictions of particle concentration profile should be compared with the experiments to ensure that the results are reliable.

In brief, the following steps should be followed:

1- Selecting the proper models according to the size of the particles
2- Boundary condition considerations
3- One-way coupling, if the volume ratio of particle volume to air volume is below 0.001
4- Ensuring grid independency for both continuous phase and dispersed phase
5- Ensuring sufficient numbers of particles injected
6- Ensuring the radiation effect of the heat source is considered

7- Comparing the predictions with the experiments for both continuous phase and dispersed phase.

References

"Air Quality Guidelines for Europe", second edition, 2000. WHO Regional Publications, European Series, No. 91. ISBN 92 890 1358 3. ISSN 0378-2255.

Alshawa, A., Russell, A.R., Nizkorodov, S.A, 2007. Kinetic analysis of competition between aerosol particle removal and generation by ionization air purifiers. Environmental science & technology 41, 2498–504.

Anderson, H.R., Ruggles, R., Pandey, K.D., Kapetanakis, V., Brunekreef, B., Lai, C.K.W., Strachan, D.P., Weiland, S.K., 2010. Ambient particulate pollution and the world-wide prevalence of asthma, rhinoconjunctivitis and eczema in children: Phase One of the International Study of Asthma and Allergies in Childhood (ISAAC). Occupational and environmental medicine 67, 293–300.

Baker, A.J., Williams, P.T., Kelso, R.M., 1994. Development of a robust finite element CFD procedure for predicting indoor room air motion. Building and Environment 29, 261–273.

Baturin, V., Translated by Blunn, O., 1972. Fundamentals of industrial ventilation. Oxford, UK: Pergamon Press.

Baumgartner, H., Loffler, F., Umhauer, H., 1986. Deep-Bed Electret Filters: The Determination of Single Fiber Charge and Collection Efficiency. IEEE Transactions on Electrical Insulation EI-21, 477–486.

Baumgartner, H.P., Löffler, F., 1986. The collection performance of electret filters in the particle size range 10 nm-10 μm. Journal of Aerosol Science 17, 438–445.

BIPM, I., ILAC, I., & ISO, I. (2008). Evaluation of Measurement Data—Guide to the Expression of Uncertainty in Measurement GUM 1995 with minor corrections.

Boor, B.E., Siegel, J.A., Novoselac, A., 2013. Monolayer and Multilayer Particle Deposits on Hard Surfaces: Literature Review and Implications for Particle Resuspension in the Indoor Environment. Aerosol Science and Technology 47, 831–847.

Bräuner, E.V., Forchhammer, L., Møller, P., Barregard, L., Gunnarsen, L., Afshari, A., Wåhlin, P., Glasius, M., Dragsted, L.O., Basu, S., Raaschou-Nielsen, O., Loft, S., 2008. Indoor particles affect vascular function in the aged: an air filtration-based intervention study. American journal of respiratory and critical care medicine 177, 419–25.

Bräuner, E.V., Forchhammer, L., Møller, P., Simonsen, J., Glasius, M., Wåhlin, P., Raaschou-Nielsen, O., Loft, S., 2007. Exposure to ultrafine particles from ambient air and oxidative stress-induced DNA damage. Environmental health perspectives 115, 1177–82.

Brown, J., Cook, K., 1950. Influence of Particle Size upon the Retention of Particulate Matter in the Human Lung*†. American Journal of Public Health 45, 450-58.

Brown, R., 1993. Air filtration: an integrated approach to the theory and applications of fibrous filters. Oxford, UK: Pergamon Press. 272 p.

Buyevich, Y., 1971. Statistical hydromechanics of disperse systems Part 1. Physical background and general equations. Journal of Fluid Mechanics. 49 (3), 489-507.

Buyevich, Y., 1972a. Statistical hydromechanics of disperse systems. Part 2. Solution of the kinetic equation for suspended particles. Journal of Fluid Mechanics. 52 (2), 352-355.

Buyevich, Y., 1972b. Statistical hydromechanics of disperse systems. Part 3. Pseudo-turbulent structure of homogeneous suspensions. Journal of Fluid Mechanics. 56, 313-336

Carvalho, T.C., Peters, J.I., Williams, R.O., 2011. Influence of particle size on regional lung deposition--what evidence is there? International journal of pharmaceutics 406, 1–10.

Crowe, C.T. (Ed.), 2005. Multiphase Flow Handbook, in: Multiphase Flow Handbook. CRC Press.

Crowe, C.T., Schwarzkopf, J., Sommerfeld, M., Tsuji, Y., 2011. Multiphase flows with droplets and particles. CRC press.

Destaillats, H., Chen, W., Apte, M.G., Li, N., Spears, M., Almosni, J., Brunner, G., Zhang, J., Fisk, W.J., 2011. Secondary pollutants from ozone reactions with ventilation filters and degradation of filter media additives. Atmospheric Environment 45 (21), 3561-3568.

Edwards, R., Jurvelin, J., Koistinen, K., 2001. VOC source identification from personal and residential indoor, outdoor and workplace microenvironment samples in EXPOLIS-Helsinki, Finland. Atmospheric Environment 35 (28), 4829-4841.

Fan, Z., Lioy, P., Weschler, C., Fiedler, N., Kipen, H., Zhang, J., 2003. Ozone-Initiated Reactions with Mixtures of Volatile Organic Compounds under Simulated Indoor Conditions. Environmental Science & Technology 37, 1811–1821.

Friedlander, S., 2000. Smoke, dust, and haze. Vol. 198. New York: Oxford University Press.

Gao, N.P., Niu, J.L., 2007. Modeling particle dispersion and deposition in indoor environments. Atmospheric Environment 41, 3862–3876.

Grabarczyk, Z., 2001. Effectiveness of indoor air cleaning with corona ionizers. Journal of Electrostatics 51-52, 278–283.

Guha, A., 2008. Transport and Deposition of Particles in Turbulent and Laminar Flow. Annual Review of Fluid Mechanics 40, 311–341.

Heiselberg, P., Sandberg, M., 1990. Convection from a slender cylinder in a ventilated room. In proceedings of Roomvent.

Hubbard, H.F., Coleman, B.K., Sarwar, G., Corsi, R.L., 2005. Effects of an ozone-generating air purifier on indoor secondary particles in three residential dwellings. Indoor air 15, 432–44.

Ibald-Mulli, A., Wichmann, H.-E., Kreyling, W., Peters, A., 2002. Epidemiological evidence on health effects of ultrafine particles. Journal of aerosol medicine : the official journal of the International Society for Aerosols in Medicine 15, 189–201.

Jacobsen, T.V., Nielsen, P.V., 1992. Velocity and temperature distribution in flow from an inlet device in rooms with displacement ventilation. Aalborg University.

Japuntich, D.A., Stenhouse, J.I.T., Liu, B.Y.H., 1994. Experimental results of solid monodisperse particle clogging of fibrous filters. Journal of Aerosol Science 25, 385–393.

Kappos, A.D., Bruckmann, P., Eikmann, T., Englert, N., Heinrich, U., Höppe, P., et al. 2004. Report The German view Health effects of particles in ambient air 207. International Journal of Hygiene and Environmental Health 207 (4), 399-407.

Kittelson, D., 1998. Engines and nanoparticles: a review. Journal of Aerosol Science 29 (1-2), 575-588.

Knol, A.B., de Hartog, J.J., Boogaard, H., Slottje, P., van der Sluijs, J.P., Lebret, E., Cassee, F.R., Wardekker, J.A., Ayres, J.G., Borm, P.J., Brunekreef, B., Donaldson, K., Forastiere, F., Holgate, S.T., Kreyling, W.G., Nemery, B., Pekkanen, J., Stone, V., Wichmann, H.-E., Hoek, G., 2009. Expert elicitation on ultrafine particles: likelihood of health effects and causal pathways. Particle and fibre toxicology 6, 19.

Knudsen, H.N., Kjaer, U.D., Nielsen, P.A., Wolkoff, P., 1999. Sensory and chemical characterization of VOC emissions from building products: impact of concentration and air velocity. Atmospheric Environment 33, 1217–1230.

Loth, E., 2000. Numerical approaches for motion of dispersed particles, droplets and bubbles. Progress in Energy and Combustion Science 26, 161–223.

Maxey, M.R., 1983. Equation of motion for a small rigid sphere in a nonuniform flow. Physics of Fluids 26, 883.

Menzel, D., 1984. Ozone - an overview of its toxity in man and animals 13, 183–204.

Mundt, E., 1996. The performance of displacement ventilation systems: experimental and theoretical studies.

Nazaroff, W., 2000. Effectiveness of air cleaning technologies. Proceedings of Healthy Buildings. In proceedings of Healthy Buildings 2, 49-54.

Nazaroff, W.W., 2004. Indoor particle dynamics. Indoor air 14 (s7), 175–183.

Neidell, M.J., 2009. Information, avoidance behavior, and health effect of ozone on asthma hospitalizations Journal of Human Resources, 44 (2), 450–478.

Nielsen, P.V., 1994. Prospects for computational fluid dynamics in room air contaminant control.

Nielsen, P.V., Allard, F., Awbi, H., Davidson, L., Schälin, A., 2007. Computational Fluid Dynamics in Ventilation Design REHVA Guidebook No 10. REHVA: Federation of European Heating and Air-Conditioning Associations.

Nielsen, P. V., 1993. Displacement ventilation-theory and design. Aalborg University.

Niu, J., 2001. Ozone emission rate testing and ranking method using environmental chamber. Atmospheric Environment 35, 2143–2151.

Niu, J., Tung, T., Burnett, J., 2001. Ozone emission rate testing and ranking method using environmental chamber. Atmospheric environment 35 (12), 2143-2151.

Offermann, F.J., Sextro, R.G., Fisk, W.J., Grimsrud, D.T., Nazaroff, W.W., Nero, A.V., Revzan, K.L., Yater, J., 1985. Control of respirable particles in indoor air with portable air cleaners. Atmospheric Environment (1967) 19, 1761–1771.

Payatakes, A.C., 1977. Model of transient aerosol particle deposition in fibrous media with dendritic pattern. AIChE Journal 23, 192–202.

Payatakes, A.C., Tien, C., 1976. Particle deposition in fibrous media with dendrite-like pattern: A preliminary model. Journal of Aerosol Science 7, 85–100.

Pekárek, S., 2003. Non-Thermal Plasma Ozone Generation. Acta Polytech 43(6), 47-51.

Penttinen, P., Timonen, K.L., Tiittanen, P., Mirme, A., Ruuskanen, J., Pekkanen, J., 2001. Ultrafine particles in urban air and respiratory health among adult asthmatics. European Respiratory Journal 17, 428–435.

Roache, P.J., 1994. Perspective: A Method for Uniform Reporting of Grid Refinement Studies. Journal of Fluids Engineering 116, 405.

Rohr, AC, Weschler, CJ, Koutrakis, P, 2003. Generation and quantification of ultrafine particles through terpene/ozone reaction in a chamber setting. Aerosol Science & Technology, 37 (1), 65–78.

Seinfeld, J. & Pandis, S. (1997). Atmospheric chemistry and physics: from air pollution to climate change. John Wiley & Sons.

Shaughnessy, R.J., Sextro, R.G., 2006. What is an effective portable air cleaning device? A review. Journal of occupational and environmental hygiene 3 (4), 169–81.

Simonin, O., Deutsch, E., Minier, J., 1993. Eulerian prediction of the fluid/particle correlated motion in turbulent two-phase flows. Springer Netherlands, 275-283.

Singer, B.C., Coleman, B.K., Destaillats, H., Hodgson, A.T., Lunden, M.M., Weschler, C.J., Nazaroff, W.W., 2006. Indoor secondary pollutants from cleaning product and air freshener use in the presence of ozone. Atmospheric Environment 40, 6696–6710.

Skistad, H., Mundt, E., Nielsen, P. V, 2004. Displacement Ventilation in Non-industrial Premises, Second. ed. Rehva.

Song, S., Lee, K., Lee, Y.M., Lee, J.H., Lee, S. I, Yu, S.D., Paek, D., 2011. Acute health effects of urban fine and ultrafine particles on children with atopic dermatitis. Environmental research 111, 394–9.

Stafford, R.G., Ettinger, H.J., 1972. Filter efficiency as a function of particle size and velocity. Atmospheric Environment (1967) 6, 353–362.

Strak, M., Janssen, N.A.H., Godri, K.J., Gosens, I., Mudway, I.S., Cassee, F.R., Lebret, E., Kelly, F.J., Harrison, R.M., Brunekreef, B., Steenhof, M., Hoek, G., 2012b. Respiratory Health Effects of Airborne Particulate Matter: The Role of Particle Size, Composition, and Oxidative Potential-The RAPTES Project. Environmental health perspectives 120, 1183–9.

Sublett, J.L., 2011. Effectiveness of air filters and air cleaners in allergic respiratory diseases: a review of the recent literature. Current allergy and asthma reports 11, 395–402.

Tien, C., Wang, C.S., Barot, D.T., 1977. Chainlike formation of particle deposits in fluid-particle separation. Science, 196 (4293), 983–985.

Tung, T., Niu, J., 2005. Determination of ozone emission from a domestic air cleaner and decay parameters using environmental chamber tests. Indoor and Built Environment, 14(1), 29-37..

Tung, T.C.W., 2005. Determination of Ozone Emission from a Domestic Air Cleaner and Decay Parameters using Environmental Chamber Tests. Indoor and Built Environment 14, 29–37.

Utell, M.J., Frampton, M.W., 2000. Acute health effects of ambient air pollution: the ultrafine particle hypothesis. Journal of aerosol medicine : the official journal of the International Society for Aerosols in Medicine 13, 355–59.

Vegendla, S.N.P., Heynderickx, G.J., Marin, G.B., 2011. Comparison of Eulerian–Lagrangian and Eulerian–Eulerian method for dilute gas–solid flow with side inlet. Computers & Chemical Engineering 35, 1192–1199.

Wang, M., Lin, C.-H., Chen, Q., 2012. Advanced turbulence models for predicting particle transport in enclosed environments. Building and Environment 47, 40–49.

Waring, M.S., Siegel, J. a., Corsi, R.L., 2008. Ultrafine particle removal and generation by portable air cleaners. Atmospheric Environment 42, 5003–5014.

Weschler, C.J., Shields, H.C., 1999. Indoor ozone / terpene reactions as a source of indoor particles 33, 2301–2312.

Zhang, T., Wang, S., Sun, G., Xu, L., Takaoka, D., 2010. Flow impact of an air conditioner to portable air cleaning. Building and Environment 45, 2047–2056.

Zhang, Y., Mo, J., Li, Y., Sundell, J., Wargocki, P., Zhang, J., Little, J.C., Corsi, R., Deng, Q., Leung, M.H.K., Fang, L., Chen, W., Li, J., Sun, Y., 2011. Can commonly-used fan-driven air cleaning technologies improve indoor air quality? A literature review. Atmospheric Environment 45, 4329–4343.

Zhang, Z., Chen, Q., 2007. Comparison of the Eulerian and Lagrangian methods for predicting particle transport in enclosed spaces. Atmospheric Environment 41, 5236–5248.

Zhao, B., Zhang, Y., Li, X., Yang, X., Huang, D., 2004. Comparison of indoor aerosol particle concentration and deposition in different ventilated rooms by numerical method. Building and Environment 39, 1–8.

Zhou, Jiaqing, Deng, Baoqing, Kim, Chang, N., 2009. Numerical Simulation of VOCs Distribution with an Air Cleaner in a Classroom, in: International Conference of Industrial Ventilation. 998–1003.

Zwick, H., Popp, W., Wagner, C., Reiser, K., Schmöger, J., Böck, A., Herkner, K., Radunsky, K., 1991. Effects of ozone on the respiratory health, allergic sensitization, and cellular immune system in children. 144, 1075–1079.

Research Articles

Paper II. Comparing the Performance of a New Electrical Aerosol Detector with other Counters

Siamak Rahimi Ardkapan, Alireza Afshari, Niels C. Bergsøe

In the Proceedings of *Indoor Air* conference, 2011

Comparing the Performance of a New Electrical Aerosol Detector with other Counters

Siamak Rahimi Ardkapan[1,*], Alireza Afshari[1], Niels C. Bergsøe[1]

[1] Department of Energy and Environment, Danish Building Research Institute, Aalborg University, DK-2980 Hørsholm, Denmark.

[*] *Corresponding email: Sra@sbi.dk*

SUMMARY

UFPs are known to be harmful to the human respiratory system. Therefore, measuring the concentration of UFPs is common in research areas related to human health. Different technologies exist for measuring the number and size of particles. In the present study, a new electrical aerosol detector was compared with two other particle measuring technologies, scanning mobility particle sizer and condensation particle counter. An electrical aerosol detector charges particles and later counts them according to their electrical movement. The particle counters were tested in a clean room with clean supply air. The results showed that the three counters follow a similar pattern at a low level of particle concentrations. An exponential relationship was found between the electrical aerosol detector and the scanning mobility particle sizer for high concentrations of particles. The condensation particle counter showed a lower particle concentration i.e. around 100,000 particles per cm^3 at high concentrations.

IMPLICATIONS

Particles are harmful to the human body and counting them in various environments is important. Also, it is important that the results obtained are reliable. A large portion of particles in the air are UFPs that can enter and stay firmly fixed deep in the human respiratory system. So, it is necessary to have reliable knowledge on the level of UFPs. The study showed that different technologies counted differently; however, all three technologies were relevant depending on their application.

KEYWORDS

Particle counter; Electric charging; Electrical aerosol detector

INTRODUCTION

Since the beginning of the last century, because of developing the welfare state of people, lifestyles were changed and consequently lead to increasing energy consumption. Using the huge volume of fossil fuels to satisfy the demands of transport, industry and buildings, new issues arose like air pollution in the big cities. The air pollution caused different problems like adverse health effects and therefore air pollutants needed more attention.

Pollution of the air includes two main types, gases and particles. Particles are added to the air by different pollutant sources like engines, stoves, etc. In addition there are different natural particle sources such as sea salts carried by the wind from the seas. Particles are also generated inside buildings by building materials.

People spend most of their time inside buildings and consequently the quality of the indoor air is important. According to research studies, particles can cause poor indoor air quality. They are divided according to their size into coarse, fine and UFPs. UFPs (UFP) are produced in the air by nucleation, combustion and other chemical reactions. In highly polluted areas of big cities, the number of UFPs is much higher than less polluted areas, because of high number of UFPs emitted by cars (Kittelson, 1998). The higher number of UFPs result in a poorer air quality and consequent adverse health effects on human (Kappos et al. 2004). So, counting the number of UFPs is of high importance. Studies show that the effect of UFPs on human health is stronger than that of other particles (Oberdörster et al. 1994).

Different technologies have been introduced for counting the concentration of particles including UFPs. The electrical aerosol detector uses electrical charge for counting particles. First it neutralises the particles of the air which passes through the counter. Next it applies a specific electrical charge to the particles and later counts them according to the electrical mobility of the particles.

Another technology is Condensation Particle Counter (CPC) that uses butanol or water for counting particles. The liquid is converted to saturated gas, which condenses on the surface of the particles. The condensed liquid droplets can be counted by light-scattering technique afterwards.

Scanning Mobility Particle Sizer (SMPS) is a technology that uses both electrical charge and condensation particle counting technology. The technology classifies the particles according to their sizes by electrical charge and later counts every size with high accuracy by applying the method of condensation particle counter. The device is not portable compare to the two previous particle counters.

The objective of this study was to compare the new UFP counter with two others. In order to ascertain the reliability of the data from different UFP counters, it is essential to evaluate them. The

studied particle counter is new and there is not enough knowledge about the reliability of data collected by the counter.

METHODS

Three particle counters were used in this study. A new Electrical Aerosol Detector called NanoTracer, PNT1000 (Koninklikjke Philips Electronics N.V.) was compared with Scaning Mobility Particle Sizer and Condensation Particle Counter, TSI model 3007. The NanoTracer is able to detect the total number of particles ranging between 10 and 300 nano meters (nm) with a concentration range of $0\text{-}10^6$ UFPs/cm^3. The other device, the SMPS counts particles with a diameter range of 7- 1000 nm. The SMPS was considered to be an immovable device. The instrument, CPC 3007, measures UFPs between 10 nm and 1 micro meter (µm) with a concentration range of $0\text{-}10^5$ UFPs/cm^3.

The measurements of particle concentration were carried out in a clean room with low particle concentration compared with ordinary residential buildings. The particle counters were settled in a clean room with the dimensions of 5.2m×2m×2.9 m. The walls of the clean room were made of steel and glass. Two displacement low velocity units have been used for supply air and the air change rate of the room was about 3 h^{-1}.

The mesurements included two parts. In the first part of the study, the NanoTracer was compared with SMPS. In the first step, the measurement was carried out when both counters were turned on simultaneously and recorded data during a period of eight hours. In the second step, first increasing the number of particles until 20,000 (counted by SMPS) and then reducing it, was done to evaluate the sensitivity of the electrical aerosol detector. The measurement was repeated twice to make sure of the results. The NanoTracer was also compared with the SMPS in a situation where the concentration of UFPs was as high as in ordinary residential buildings. A pure-wax candle was used to generate the particles. The candle burned for 30 minutes. The level of UFP was measured continuously during the measurement.

In the second part, the NanotTracer was compared with the CPC. In the first step, both counters were turned on while the concentration was low to compare the two counters in the low concentration of UFPs. They were turned on, and then the counters measured the number of UFPs continuously for two hours. In the second step, a candle was used to generate a high concentration of UFPs. The candle burned for 30 minutes. The level of UFPs was counted continuously by the two counters.

RESULTS

The first part of the measurements was to compare the SMPS and the NanoTracer. In the first step of the measurements, the NanoTracer, and the SMPS were used to log the data on a low

concentration of UFPs. As shown in Figure 1, both devices showed almost the same results for the case of low level of UFPs. However, the fluctuation of the NanoTracer was higher than the SMPS. The calculated average data for the NanoTracer was 600 UFP/cm^3, while the number was 900 for SMPS.

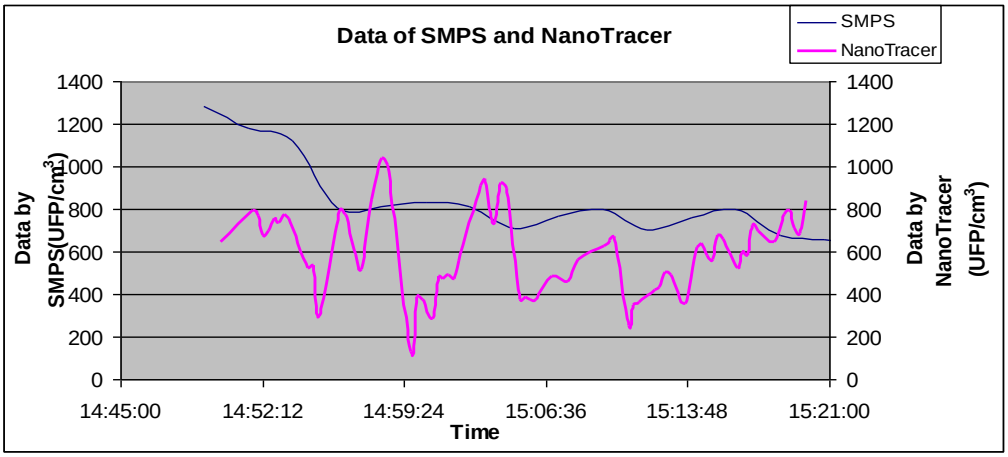

Figure 1. Comparison of registered data of the NanoTracer with SMPS for a low level of UFP

In the second step, small changes occurred in the number of UFPs. The result is shown in Figure 2. SMPS showed a trend of decreasing the number of UFPs and it showed a small peak at the time of 15:30. However, the data provided by the NanoTracer showed a lot of fluctuations averaging 500 UFPs/cm^3. On the other hand the data of the SMPS started at 20,679 UFPs/cm^3 and the final number recorded was 47 UFPs/cm^3. The average of all data recorded by recorded SMPS was 1775 UFPs/cm^3.

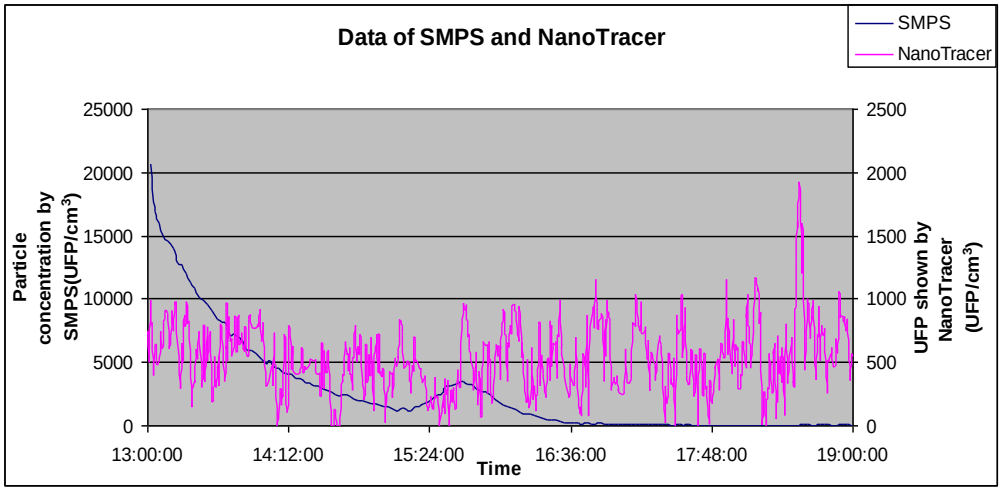

Figure 2. Comparison of the data of the NanoTracer with recorded SMPS at changing UFP

At this step, the high concentration of the particles was generated by a burning candle. The data of the particle counters are shown in Figure 3. The horizontal axis is related to SMPS data, while the vertical axis represents NanoTracer data. The trendline for the curve is an exponential equation with the R2 of about 0.9.

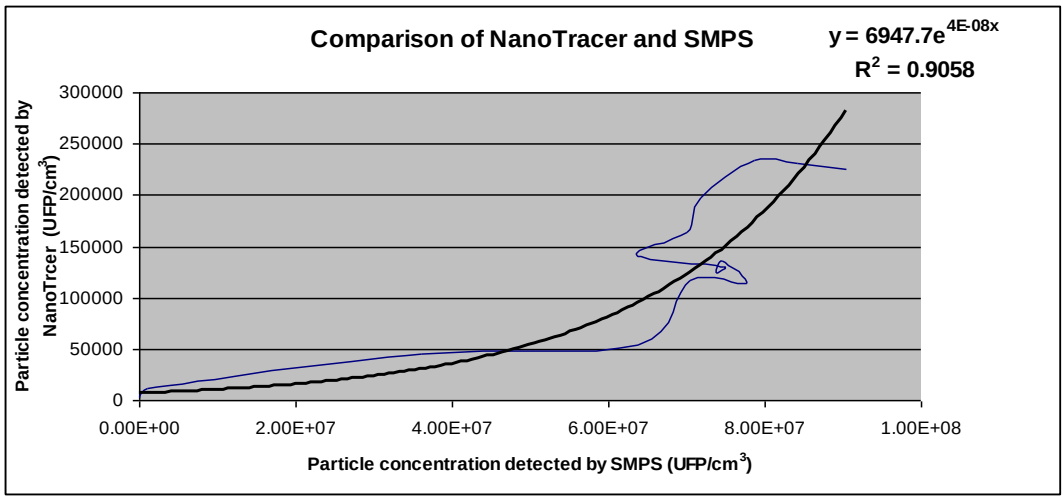

Figure 3. Comparison of registered data of the NanoTracer with recorded SMPS at high levels of UFP

The second part of the measurements consisted of comparing the NanoTracer with the condensation particle counter (CPC). At the first step, a low level of UFPs was compared. As it is shown in Figure 4, the detected data of both counters showed the same shape but with different levels.

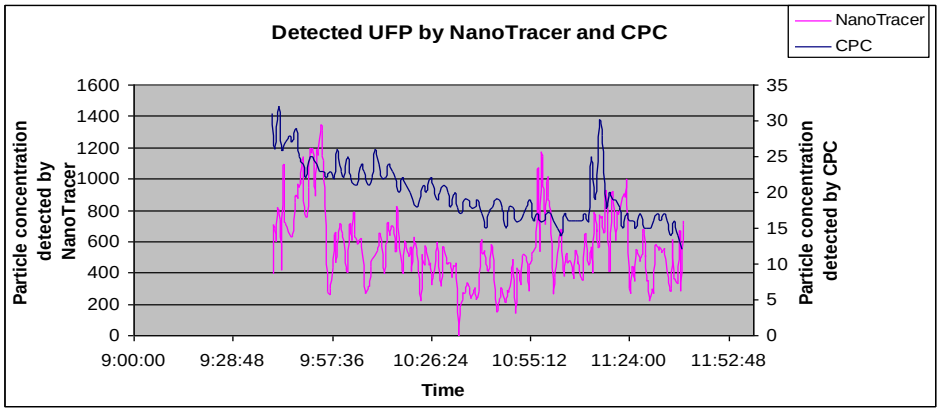

Figure 4. Comparison of registered data of the NanoTracer with CPC for a low concentration of UFP

The data of the CPC showed a smaller number compared with the NanoTracer data. The data of both counters are related by the following equation:

$$Y = X + 510 \pm R \tag{1}$$

The variable X shows the data of theCPC and Y shows calculated data for the NanoTracer. The average error is shown by R, which equals 179.

As shown in Figure 5, the results related to a high concentration of UFPs showed that the data of CPC and NanoTracer follow the same trace until concentration of about 90,000 UFPs. The relation between is linear and it is:

$$N = 0.3643C + 32559 \tag{2}$$

Were N is the number shown by the NanoTracer and C is the number shown by the CPC.

After that a discrepancy between the results of the two counting devices became obvious. The data shown by the CPC were almost constant while the NanoTracer showed an increased number of particles.

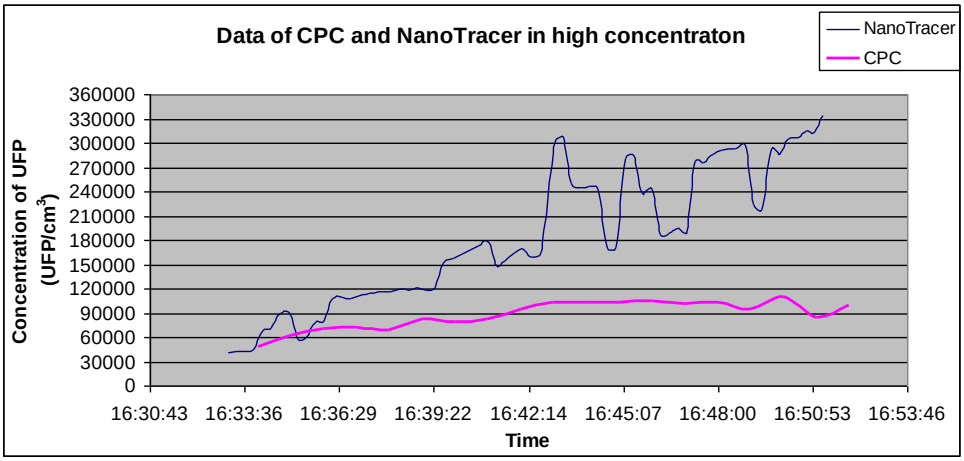

Figure 5. Comparison of the data of the NanoTracer with the CPC at high concentrations of UFP

DISCUSSION

A new electrical aerosol detector was compared with two other counters. First, the detector was compared with the SMPS. In a low concentration as shown in Figure 1, the data logged by both counters were similar. By decreasing the ultrafine concentration, as shown in Figure 2, the NanoTracer did not show the right number but showed a number of fluctuations close to the previous level. The possible reason could be that the resolution of the device for the concentration which is ± 1500 UFPs/cm^3. Another possible reason could be the limitation of the diameter range that the electrical aerosol detector could detect.

In the case of higher concentrations, the logged data of the both UFP counters showed an increased number of UFPs. However, they did not show the same number for this case. Figure 3 shows the data of the NanoTracer versus the SMPS data. The trend line best suited to the data was an exponential line with the R-squared of 90%. One possible reason could be a bigger increase in the number of particles with an out-sized diameter which NanoTracer can count.

The second part of the measurement consisted of comparing the NanoTracer with CPC. The logged data of both UFP counters are shown in Figure 3. The data of the condensation particle counter (CPC) showed a smaller number compared with the NanoTracer data. However, the fluctuations of the UFP concentration logged by the two counters were similar and the data of the NanoTracer is related to the data of CPC with a linear equation as shown in Equation (1).

In addition, with high concentration of UFPs, the logged data of NanoTracer and the CPC were to some extent the same. Then after about 90,000 UFPs, as we can see in Figure 5, the NanoTracer showed a higher number than the CPC. It seems that the main reason for the discrepancy between the data of the CPC and the NanoTracer was due to the counting limitations of the CPC after 100,000 UFPs/cm^3.

CONCLUSIONS

Three particle counters were evaluated in this study. At low level of UFPs, the results of the three counters were similar. In the case of small changes in the number of UFPs, the NanoTracer did not show clearly the change, while the SMPS did. At a high level of UFPs, logged data of the NanoTracer and the SMPS were related by an exponential equation. The possible reason could be the wider diameter range of the SMPS compared with the NanoTracer. With the concentration higher than 90,000, the NanoTracer presented more reliable results than the CPC. The reason seems to be the existing limitation by the CPC for the maximum concentration. The three counters are useful depending on the application. In the case of measuring the pollution of ordinary residential buildings, the NanoTracer was found to be reliable. In the case of studying small changes in the concentration of UFPs, the counter was found not to be reliable. It must be taken into account that it is easier to handle the NanoTracer than the two other particle counters. The SMPS has the biggest size and it needs to be kept in a fixed horizontal position during the measurement. The NanoTracer works continuously in all positions. Its size is also smaller than the two others, so its handling is easier than that of the two other particle counters.

ACKNOWLEDGEMENT

The authors gratefully acknowledge the financial support given by ELFORSK, the Danish energy programme of research and development in energy efficiency.

REFERENCES

Kittelson D.B., 1998. Engines and nanoparticles: a review. In Proceeding of: Journal of Aerosol Science 29, pp. 575-588.

Kappos A. D., Bruckmann P., Eikmann T., Englert N., Heinrich U., Höppe P., Koch E., Krause G. H.M., Kreyling W. G., Rauchfuss K., Rombout P., Schulz-Klemp V., Thiel W. R., . Wichmann H. E. 2004. International Journal of Hygiene and Environmental Health, 207(4), pp. 399-407.

Oberdörster G., Ferin J., Lehnert B.E. 1994. Correlation between particle size, in vivo particle persistence, and lung injury. In Proceeding of: Journal of Environmental Health Perspective 102(5), pp. 173-179.

Paper V. Simulation of particle distribution in a room with air cleaner

Siamak Rahimi Ardkapan, Alireza Afshari, Peter V. Nielsen, Ahsan Iqbal, Niels C. Bergsøe

In the proceedings of *Healthy Building* conference, 2012

Simulation of particle distribution in a room with air cleaner

Siamak Rahimi Ardkapan[1], Alireza Afshari [1], Peter V. Nielsen [2], Ahsan Iqbal[1], Niels C. Bergsøe[1]

[1]Department of Energy and Environment, Danish Building Research Institute, Aalborg University, DK-2970, Hørsholm, Denmark
[2]Department of Civil Engineering, Aalborg University, DK-9000 Aalborg, Denmark

[*]*Corresponding email: sra@sbi.dk*

SUMMARY

Ventilation is one of the ways that humans can keep the indoor air quality at the proper level. Portable air cleaners have been developed to improve indoor air quality while reducing the energy consumption of the ventilation system. The aim of this study is to find the correct turbulence model and particle phase model for simulating an air cleaner in a room. In addition, the aim is to study the impact of location of an air cleaner in a room. The dynamics of the particle inside a room was simulated by computational fluid dynamics software. Furthermore, the air change rate was measured by both tracer gas and particles with different sizes. The proper turbulence model was selected after comparing the results with the behaviour of the gas in the test room. The simulations showed the effect that the location of an air cleaner had on the particle level. The results showed that the location of the air cleaner in relation to inlet, outlet and particle source had a significant effect on the effectiveness of the air cleaner.

Keywords: Air cleaning; Particle dynamics; Particles; Computational Fluid Dynamics; Turbulence Models

1 INTRODUCTION

The purpose of a ventilation system is to supply heating, cooling and clean air to the residents of buildings. For years, computational fluid dynamics (CFD) has been used for simulating ventilation systems. It has included simulating the behaviour of gases and particles. Mainly, there are two models for simulating the pollutants including particles, the Eulerian model and the Lagrangian model.

The Eulerian model assumes that the behaviour of the particle phase is a continuum, while the Lagrangian model coupled with the point-force approach considers the particles as single points (Crowe, 2006). Various studies have been conducted on the particle phase models combined with different turbulence models for different particle sizes (Wang et al., 2011). In most studies, the simulated particle sizes are in the range of fine particles or coarse particles, i.e. particles larger than 100 nm.

The aim of this evaluation was to simulate the behaviour of particles including UFPs, i.e. particles smaller than 100 nm. In addition, the aim was to study the discrepancy of the Lagrangian model compared with the real measurements. Moreover, the effect of the location of an air cleaner on its effectiveness was assessed.

2 METHODOLOGY

In this study, a real room was simulated by CFD software, STAR-CCM+. The meshes were generated by both polyhedral meshing and prism layer meshing. The quality of mesh was improved sufficiently to achieve a grid-independent solution. To select the proper turbulence model, the air movement from the inlet was visualised by smoke in a test room. Thereafter, the simulation was run with the turbulence models, K-epsilon and K-omega. In order to simulate the behaviour of particles, the Lagrangian multiphase was selected. Next, an air cleaner was added to the simulation. Three different locations of the air cleaner were simulated.

In the test room, the tracer gas N_2O was used to measure the ventilation rate of the room. A photo-acoustic gas monitor was used for measuring the tracer gas. For different sizes of particles, Scanning Mobility Particle Sizer (SMPS) was used to count the number of particles for each size. The SMPS could count sizes from 7 nm to 1000 nm. The particles were generated by a burning pure wax candle. The decay rate of different particle sizes was calculated and then the decay rates were compared with the tracer gas decay. The size of simulated particles was determined to be normal distribution according to the results of SMPS.

3 RESULTS

First, the results of measurements will be shown. The tracer gas, N_2O, was released inside the room and the decay of the tracer gas was measured to be 1.6 h^{-1}. Particles were generated by a candle in the room and the decay rate of particles was measured by SMPS. According to the results of the SMPS, different particle sizes had different decay rates in the room. As shown in Figure 1, particles with a diameter of less than 73 nm had a higher decay rate than the decay rate of the tracer gas, while particles larger than this size had a lower decay rate than the decay rate of tracer gas. Moreover, the fine particles had a similar decay rate compared with the tracer gas decay rate. Therefore, assuming particle behaviour identical to the behaviour of tracer gas does not give large inaccuracy. Particles smaller than 73 nm have a higher decay rate than the tracer gas decay rate.

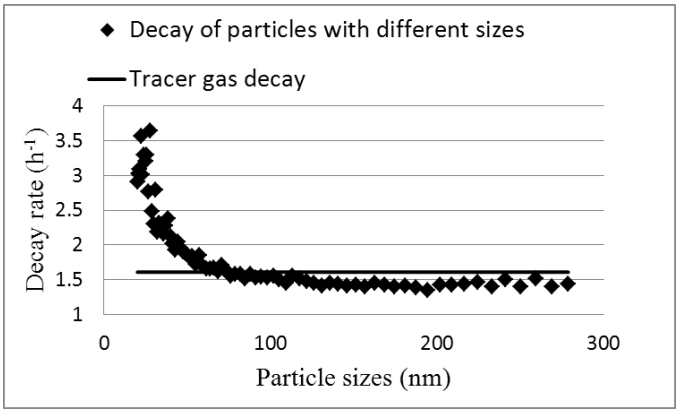

Figure 1. Decay rate of particles compared with the decay rate of tracer gas.

The weighted mean for the decay rate of whole particles was determined by averaging the decay rate of the particles with different sizes by considering the number of every size. The weighted mean decay rate for the particles was 1.63 (h^{-1}), which was very close to the number given by tracer gas decay rate, i.e. 1.61 (h^{-1}).

The measurement showed that the weighted mean of the decay rate of particles was almost the same as the decay rate of the tracer gas. However, different sizes of particles showed different decay rates. In this study, the Lagranigian method was used for the case simulating different sizes of particles in the room. The size of particle was considered a normal distribution that is determined according to the results of the SMPS.

The simulation was run to select a proper turbulence model for the case study. The results of the K-epsilon and K-omega models were compared with the behaviour of air in the real room. As indicated in Figure 2, the smoke visualizations showed that the K-epsilon model matched the real case the best. After entering the room, the air dropped down after 20 cm due to temperature difference. The temperature of the test room was 2 degrees higher than the supply air. The dimensions of the inlet was 4×52 cm and the inlet velocity of the air was 0.3m/s. The K-epsilon model showed the same behaviour of the real flow, while the K-omega model showed that the air first reached the floor close to the opposite wall.

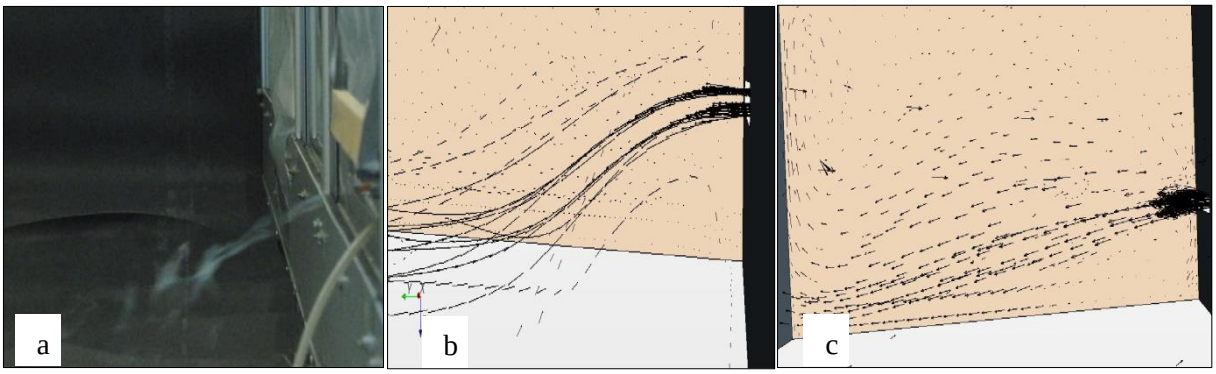

Figure2. Smoke visualisation and simulation results a) smoke, b) K-epsilon, c) K-omega.

The velocity profile predicted by K-epsilon and K-omega models was compared with the measured velocity in the room in Figure 3. As seen from the figure, the results of simulation by the K-epsilon turbulence model showed results similar to the velocities measured in the test room. The Y axis showed the height from the floor in front of the inlet at a distance of 1m.

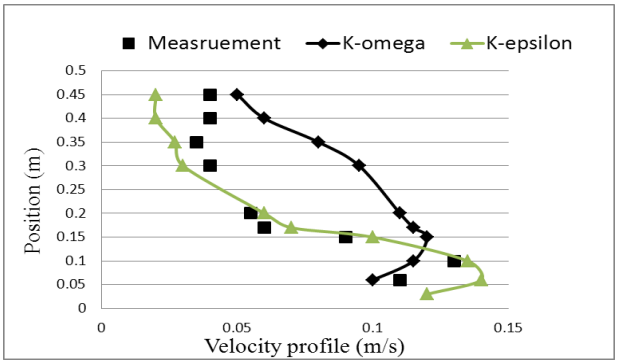

Figure 3. Prediction of velocity profile at a distance of 1 m in front of the inlet by K-epsilon and K-omega compared with the measurement results.

There are two ways of modelling the particle behaviour of the air, the Lagrangian model and the Eulerian model. In the Eulerian approach, the particles are considered as a continuum with

properties similar to the properties of a fluid. The Lagrangian multiphase model does not consider the properties of the particles similar to the fluid. Instead, it solves the equations with regard to the forces exerted by the flow to the discretised cells that contain particles. In the software, the Trajectory method was used for the Lagrangian model (Crowe, 2006).

In this study, the Lagrangian multiphase model was selected to evaluate the impact of the location of air cleaner on the particle concentration inside the room. A log normal distribution was considered for the particles with the source location similar to the candle in the real room close to the floor. The particle size distribution was determined according to the size distribution found by the SMPS measurements.

Next, the air cleaner was added to the simulation. Three different locations of the air cleaner were simulated with the K-epsilon model, while the particle movements were simulated by Lagrangian model.

As shown in Figure 4, the air cleaner was placed in three different locations. The locations were evaluated in the simulations. The first place was the remotest place from the inlet and outlet. The second location was close both to the inlet and to the outlet. The third location was at the other side of the room but close to both inlet and outlet. Therefore, the position of Location 1 is similar to that of Location 3.

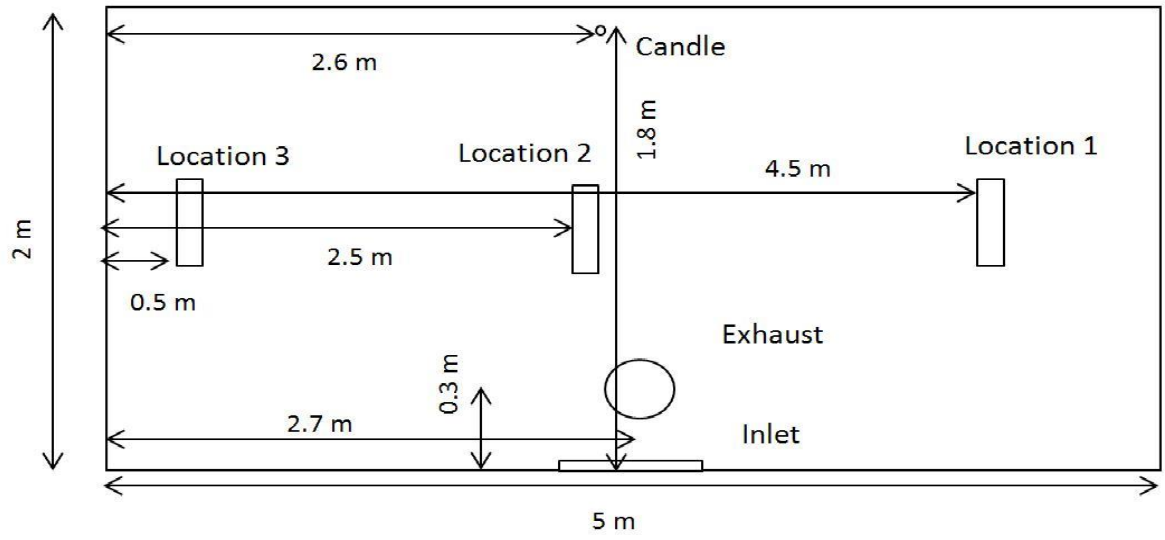

Figure 4. The locations of the air cleaner in the room.

A global value such as average particle concentration is used in the room. The average concentration of the particles in the room for the case of ventilation without air cleaner is designated C_0. The average concentration of the particle in the room for the other three cases is designated C_1, C_2 and C_3 respectively.
The improvement of the removal effectiveness for Locations 1, 2 and 3 is calculated by Equation 1.

$$I = \frac{C_0 - C_i}{C_0}\% \quad i = 1,2,3 \tag{1}$$

Where, I is the improvement in the particle removal efficiency of the ventilation system together with air cleaner, compared with the ventilation of the room alone. The result is shown in Table 1. It is seen that Location 2 had the best effectiveness. The worst effectiveness was for Location 3.

Table 1. The effectiveness of different locations for the air cleaner.

Parameter	Location 1	Location 2	Location 3
Distance to particle source (m)	2.62	1.39	2.65
Improvement by the air cleaners (%)	26	27	23

4 DISCUSSION

As shown in Figure 1, the decay rate of fine particles was similar to the tracer gas decay rate and the figure confirmed that for UFPs there was a great difference between the decay rate of tracer gas and the decay rate of UFPs. This means that it is possible to use both the Lagrangian model and the Eulerian model for the same size of fine particles (Zhang and Chen, 2006).

However, for UFPs the faster decay of UFPs must be taken into account. The main reasons for the faster decay rate of UFPs are agglomeration and coagulation which must be handled in the simulation separately. More investigations will be done concerning this phenomenon to determine the best multiphase model for predicting the behaviour of UFPs in the simulation.

Two of the frequently used turbulence models are K-epsilon and K-omega. After evaluating the results of the simulations with both models for the real room in a laboratory environment, it was proven that for this case the K-epsilon model predicts the flow most accurately. Therefore, it was used for the rest of the simulations.

The location of an air cleaner has only a small impact on the average particle concentration. Changing the location of the air cleaner will change the air distribution in the room and consequently it changes the average particle concentration in the room.

5 CONCLUSION

It is concluded that to determine the exact behaviour of the whole range of particles, the behaviour of UFPs needs to be studied and then to be simulated in CFD. It is also concluded that the location of an air cleaner can have a small impact on the effectiveness of an air cleaner.

ACKNOWLEDGEMENT

The authors gratefully acknowledge the support of ELFORSK, the Danish energy programme of research and development in efficient energy use. Also, we highly appreciate the cooperation of the Copenhagen Center for Atmospheric Research.

6 REFERENCES

Crowe C.T. 2006.Multiphase flow handbook. Taylor & Francis, Boca Raton, Fl.
Wang M, Lin C, and Chen Q. 2012. Advanced turbulence models for predicting particle transport in enclosed environment. Building and Environment, 47(2012), 40-49.
Zhang Z. and Chen Q. 2007.Comparison of the Eulerian and Lagrangian methods for predicting particle transport in enclosed spaces. Atmospheric Environment, 41, 5236-5248.